Research Square

Preprints are preliminary reports that have not undergone peer review.
They should not be considered conclusive, used to inform clinical practice,
or referenced by the media as validated information.

Pasteurized probiotic fermented milk Attenuates DSS-Induced-Colitis via modulation of specific intestinal metabolites

Lu Gao
Inner Mongolia Agricultural University
Hongliang Li
Inner Mongolia Mengniu Dairy (Group) Co., Ltd.
Luping Yang
Inner Mongolia Agricultural University
Chang Yang
Inner Mongolia Mengniu Dairy (Group) Co., Ltd.
Xinxue Zhao
Inner Mongolia Agricultural University
Guohong Wang
Inner Mongolia Mengniu Dairy (Group) Co., Ltd.
Xueli Li
Inner Mongolia Mengniu Dairy (Group) Co., Ltd.
Meng Zhang
Inner Mongolia Agricultural University
Zhihong Sun
Inner Mongolia Agricultural University
Heping Zhang
Inner Mongolia Agricultural University
Feiyan Zhao
15754881670@163.com

Inner Mongolia Agricultural University

Article

Keywords: IBD (Inflammatory Bowel Disease), Pasteurized probiotic fermented milk, metabolites, Inflammatory levels, Multi omics

Posted Date: September 11th, 2026

DOI: https://doi.org/10.21203/rs.3.rs-10668167/v1

License: This work is licensed under a Creative Commons Attribution 4.0 International License.
Read Full License

Additional Declarations: No competing interests reported.

Pasteurized probiotic fermented milk Attenuates DSS-Induced-Colitis via modulation of specific intestinal metabolites

Lu Gao [1#] Hongliang Li [2,3#] Luping Yang [1] Chang Yang [2,3] Xinxue Zhao [1] Guohong Wang [2,3] Xueli Li [2,3] Meng Zhang [1] Zhihong Sun [1] Heping Zhang [1] Feiyan Zhao [1*]

([1] Inner Mongolia Key Laboratory of Dairy Biotechnology and Engineering, Key Laboratory of Dairy Products Processing, Ministry of Agriculture and- Rural Affairs, Key Laboratory of Dairy Biotechnology and Engineering, Ministry of Education, Inner Mongolia Agricultural-University, Hohhot 010018, P.R. China

[2] Inner Mongolia Mengniu Dairy (Group) Co., Ltd., Hohhot, 011500, China

[3] Mengniu Hi-Tech Dairy Products (Beijing) Co., Ltd., Beijing, 101100, China)

# These authors contributed equally to this work.

* Correspondence author

Feiyan Zhao

E mail:15754881670@*163.com*

China,Hohhot, Inner Mongolia Autonomous Region, 010010

Abstract:

Functional pasteurized fermented milk represents an important direction in dairy product development. This study investigated the alleviating effects and mechanisms of pasteurized fermented milks containing *Bifidobacterium animalis* subsp. *Lactis* Probio-M8, *Lactobacillus paracasei* PC-01, and their combination on DSS-induced IBD in mice. Metabolomics revealed that the pasteurized probiotic fermented milks were enriched in active metabolites such as organic acids and lipids, suggesting immunomodulatory potential. Animal experiments showed that they reduced the DAI and LPS levels, modulated inflammatory cytokines and oxidative stress, and repaired intestinal barrier damage. Further studies found that they restored gut microbiota dysbiosis and the levels of short-chain fatty acids and tryptophan metabolites. Moreover, different fermented milks exhibited distinct pathway regulation: the Probio-M8 and PC-01 formulations activated the AMPK pathway, while the combination formulation inhibited pathways such as IL-17 and TNF , thereby alleviating colitis.

Keywords IBD (Inflammatory Bowel Disease); Pasteurized probiotic fermented milk;

metabolites; Inflammatory levels; Multi-omics

1. Introduction

Inflammatory bowel disease (IBD) encompasses chronic, relapsing inflammatory disorders of the gastrointestinal tract, principally ulcerative colitis (UC) and Crohn's disease (CD), the etiology of which remains incompletely elucidated. The incidence of IBD has continued to increase worldwide, particularly in newly industrializing countries, in parallel with changes in lifestyle and dietary patterns[1]. Its pathogenesis arises from complex interactions among genetic susceptibility, environmental exposure, gut microbial dysbiosis, and dysregulated host immune responses[2,3]. Current clinical management primarily relies on aminosalicylates, glucocorticoids, immunosuppressants, and biological agents. Nevertheless, the long-term utility of these treatments is constrained by variable efficacy, clinically significant adverse effects, including an increased risk of infection and complications associated with sustained immunosuppression, and primary non-response or secondary loss of response in some patients[4,5]. Therefore, safe and effective adjunctive strategies suitable for long-term use are urgently needed.

The gut microbiota is a fundamental regulator of intestinal homeostasis. Microbial dysbiosis may favor the expansion and mucosal colonization of opportunistic pathogens, eliciting aberrant immune responses that contribute to IBD development and progression[6]. Clinical cohort analyses have identified an enrichment of *Parasutterella excrementihominis* in patients with UC. Monocolonization of germ-free mice with this taxon exacerbated experimental colitis, whereas its metabolites promoted neutrophil extracellular trap (NET) formation and intensified epithelial injury through reactive oxygen species (ROS) and proinflammatory mediators[7]. IBD-associated microbial disruption is accompanied by altered metabolite production. Short-chain fatty acid (SCFA)-producing taxa, including *Faecalibacterium*, *Eubacterium hallii* group, *Bifidobacterium*, *Akkermansia*, *Lachnospira*, *Ruminococcaceae*, *Lactobacillus gasseri*, and *Ruminiclostridium*, are consistently depleted in patients with IBD and murine models. These compositional changes coincide with substantial reductions in SCFA concentrations, potentially compromising the energy supply to intestinal epithelial cells[8,9]. In addition to these microbial and metabolic disturbances, IBD is characterized by persistent inflammation, impaired intestinal barrier integrity, and heightened oxidative stress. The severity and resolution of these pathological processes are strongly influenced by the composition and metabolic activity of the gut microbiota. For instance, parthenolide attenuates colonic inflammation in a microbiota-dependent manner. Its protective activity is associated with the restoration of the regulatory T-cell/T helper 17-cell (Treg/Th17) balance in the intestinal mucosa following increased production of microbiota-derived SCFA[10]. Conversely, gut dysbiosis can amplify oxidative stress and inflammation through several

mechanisms, including diminished SCFA synthesis and increased intestinal permeability[11]. Collectively, these observations provide a compelling rationale for microbiota-directed strategies that restore beneficial metabolite production as adjuncts to conventional IBD therapy. Probiotic fermented milk is a milk-based product obtained through fermentation with viable microorganisms that confer health benefits to the host[12]. Regular consumption of these products is associated with the attenuation of disease-related gut dysbiosis[13,14]. These beneficial effects are partly attributed to fermentation-derived bioactive compounds, including functional peptides and exopolysaccharides[15]. For example, milk fermented with *Lacticaseibacillus rhamnosus* GG attenuated dextran sulfate sodium (DSS)-induced intestinal injury and inflammation in mice by activating EGFR-Akt signaling and inhibiting cytokine-induced apoptosis[16]. Pasteurization after fermentation offers a complementary product development strategy. Although thermal treatment eliminates viable microorganisms, it retains bacterial cellular constituents and many fermentation-derived bioactive metabolites. Compared with live-culture fermented milk, pasteurized products are less dependent on stringent cold-chain storage and can maintain stable sensory quality at ambient temperatures. These attributes have positioned pasteurized fermented milk as a distinct category in the development of functional dairy products. Emerging evidence suggests that pasteurized fermented milk produced with probiotic strains retains health-modulating activity. For example, a multistrain formulation altered the gut microbiota, composition particularly by enriching *Bifidobacterium longum*, and increased SCFA concentrations in a cohort characterized by suboptimal health. These changes coincided with improved sleep quality and reductions in symptoms associated with suboptimal health[17]. However, evidence concerning the capacity of these products to mitigate intestinal inflammation and regulate host immune responses remains limited, and their underlying mechanisms require further investigation.

To address this knowledge gap, we selected two strains with probiotic potential and favorable fermentation characteristics. First, *Bifidobacterium animalis* subsp. *Lactis* Probio-M8 was isolated from the breast milk of a healthy donor. Previous studies have demonstrated that Probio-M8 can attenuate inflammation and enhance immune function by modulating the gut microbiota and its associated metabolic pathways or metabolites[18-20]. Incorporating it into milk fermentation also increases the concentrations of several organic acids, amino acids, and essential fatty acid-related- metabolites, thereby enhancing the sensory and nutritional properties of fermented milk[21]. The second strain, *Lactobacillus paracasei* PC-01, was isolated from Tibetan sour yak milk[22]. Milk beverage with PC-01 protects the intestinal barrier against chemical and inflammatory insults by preserving epithelial integrity and suppressing the production of pro-inflammatory cytokines and chemokines[23]. Accordingly, we prepared four pasteurized fermented milk formulations: three fermented with Probio-M8 alone, PC-01 alone, or both strains in co-culture, and a conventional control fermented with a standard dairy starter culture lacking probiotic strains. We characterized the formulations through *in vitro*

metabolomic profiling and evaluated their biological efficacy *in vivo* using a DSS-induced colitis mouse model. Metagenomic, metabolomic, and transcriptomic analyses were integrated to delineate the formulation-specific mechanisms underlying the attenuation of experimental colitis. This integrated approach was designed to provide a mechanistic and empirical foundation for developing non-refrigerated functional dairy products.

2. Materials and methods

2.1 Materials

The probiotic strains used in this study were *Bifidobacterium animalis* subsp. *Lactis* Probio-M8 (Probio-M8; GenBank accession number: CP047190) and *Lactobacillus paracasei* PC-01 (PC-01; GenBank accession no. CP063652). Dextran sulfate sodium (DSS; molecular weight, 36–50 kDa) was purchased from MP Biomedicals (Irvine, CA, USA). Six-week-old male C57BL/6J mice weighing 20–23 g and standard rodent chow and bedding were obtained from Beijing Huafukang Bioscience Co., Ltd. (Beijing, China; animal production license no. SCXK (Beijing) 2019-0014). Rabbit anti-ZO-1 (catalog no. 21773-1-AP) and anti-MUC2 (catalog no. 27675-1-AP) antibodies were purchased from Proteintech (Wuhan, China). Rabbit anti-occludin- antibody (catalog no. R15100-33) was obtained from Hangzhou Huaan Biotechnology Co., Ltd. (Hangzhou, China). Alexa Fluor 488- and 594-conjugated secondary antibodies (33106ES60) were obtained from Yeasen Biotechnology (Shanghai, China). Commercial assay kits for measuring the serum concentrations of interleukin IL-6, IL-1β, IL-17A, tumor necrosis factor-α (TNF-α), malondialdehyde (MDA), and lipopolysaccharide (LPS), as well as the concentration of superoxide dismutase (SOD) and glutathione peroxidase (GSH-Px), were purchased from Quanzhou Ruixin Biological Technology Co., Ltd. (Quanzhou, China). All assays were performed according to the manufacturer's instructions.

2.2 Preparation of pasteurized fermented milk

Four pasteurized fermented milk formulations were prepared using an identical milk base containing 93.5% raw bovine milk and 6.5% sucrose. The milk base was initially heat-treated at 95 °C for 25 s and then cooled to 42 °C. The conventional starter culture alone, starter culture supplemented with Probio-M8, starter culture supplemented with PC-01, or starter culture supplemented with both Probio-M8 and PC-01 were then inoculated. These were used to produce PRE pasteurized fermented milk (PRE formulation), Probio-M8 pasteurized fermented milk (Probio-M8 formulation), PC-01 pasteurized fermented milk (PC-01 formulation), and PM8 pasteurized fermented milk (PM8 formulation) Following inoculation, the milk base was incubated at 42 °C until the pH dropped to 4.5. Subsequently, the fermented products were subjected to a second pasteurization step at 75 °C for 25 s before being stored at ambient temperature. All four formulations were manufactured by Inner Mongolia Mengniu Dairy

(Beijing, China).

2.3 Animal experiments and ethical statement

Six-week-old male C57BL/6J mice weighing 20–23 g were used in this study. Before the experiment, the animals were acclimatized to the housing environment for seven days. They were maintained in sterilized, ventilated polycarbonate cages under controlled conditions comprising a 12-h light/12-h dark cycle and a temperature of 25 ± 2 °C, with ad libitum access to standard laboratory chow. All animal procedures complied with the Guidelines for the Care and Use of Laboratory Animals of Inner Mongolia Agricultural University (license no. SYXK-2020-0002). The experimental protocol was approved by the Animal Ethics Committee of Inner Mongolia Agricultural University (approval no. NND2025165).

2.4 DSS-induced chronic colitis model and interventions

Chronic colitis was induced by intermittent administration of 2.5% DSS in drinking water. Each 10-day cycle comprised 5 days of DSS exposure, followed by 5 days of sterile water administration. This regimen was repeated for 3 consecutive cycles, resulting in a total experimental duration of 30 days. The mice were randomly allocated to six groups (n=7 per group): untreated control (NC), model (DSS), pasteurized fermented milk without probiotic supplementation (PRE), pasteurized fermented milk supplemented with Probio-M8 (M8), pasteurized fermented milk supplemented with PC-01 (PC-01), and pasteurized fermented milk supplemented with both Probio-M8 and PC-01 (PM8). All groups, except the NC group, underwent DSS treatment, and the NC group received sterile drinking water throughout the experiment. The NC and DSS groups received saline via oral gavage at 0.2 mL/day, whereas the remaining groups received 0.2 mL/day of their respective pasteurized fermented milk formulations. At the end of the experiment, the mice were deeply anesthetized by intraperitoneal injection of 1% sodium pentobarbital (50 mg/kg). Blood was collected from the retro-orbital venous plexus under deep anesthesia, after which the mice were euthanized by cervical dislocation. Serum was separated from whole blood and stored at −80 °C until biochemical and immunological analyses. Fecal samples were collected at baseline (day 0) and at the end of the intervention (day 30), immediately frozen, and maintained at −80 °C until analysis.

2.5 Disease activity index (DAI)

Colitis severity in DSS-treated mice was assessed using the disease activity index (DAI). Based on previous literature, with some modifications. The three DAI components were scored according to the following criteria: (1) body weight loss: 0, no loss; 1, 1–5%; 2, 5–10%; 3, 10–15%; and 4, >15%; (2) occult blood or gross bleeding: 0, negative; 1, positive within 60–120 s; 2, positive within 30–60 s; 3, positive within 10–30 s; and 4, immediate positivity or gross bleeding; and (3) fecal consistency: 0, normal; 1, soft; 2, very soft; 3, diarrhea and 4, Watery

feces[24].

2.6 Histological examination of colon tissue

Colon tissues fixed in 4% paraformaldehyde were transferred to tissue-embedding cassettes and rinsed overnight under running water. The tissues were successively dehydrated in 70%, 80%, and 90% ethanol for 5 min each, followed by two 5-min changes each in 95% ethanol and absolute ethanol. The dehydrated tissues were subsequently cleared in xylene, infiltrated twice with molten paraffin over a total period of 4 h, and embedded with the luminal surface oriented downward. Serial sections measuring 8μm in thickness were cut, floated on a water bath maintained at 45 °C, collected on glass slides, and dried at 37 °C. For hematoxylin and eosin staining, the sections were deparaffinized in xylene and rehydrated sequentially with 100%, 90%, 75%, and 50% ethanol for 10 min at each concentration. Subsequently, they were immersed in distilled water for 5 min and washed three times with 0.01 M phosphate-buffered saline (PBS; pH 7.4) for 15 min per wash. Each section was covered with one drop of hematoxylin solution and stained for 10 min at room temperature. The sections were then rinsed with tap water to induce the bluing process. After three additional 15-min washes with PBS, one drop of alcohol-soluble eosin solution was applied to each section for 1 min at room temperature, followed by rinsing with tap water. The stained sections were dehydrated in absolute ethanol for 5 min, cleared through two 20-min changes of xylene, and mounted with neutral balsam. Colonic morphology was examined using light microscopy, and digital images were acquired. Histopathological alterations were graded according to established scoring criteria to quantify the severity of colonic tissue injury[25].

2.7 Immunofluorescence staining

Colon sections were processed using two independent immunofluorescence protocols: dual ZO-1+MUC2 and single occludin staining. Both protocols incorporated identical pre-treatment procedures. After equilibration to room temperature, the sections were fixed with 4% paraformaldehyde and washed with PBS. They were then incubated sequentially with permeabilization solution, 3% H_2O_2, and blocking solution at room temperature, with PBS washes between successive treatments. For dual ZO-1+MUC2 staining, the blocked sections were incubated with an anti-ZO-1 primary antibody (1:2000) overnight at 4 °C. After washing with PBS, the sections were incubated with Alexa Fluor 488-conjugated secondary antibody (1:200) at 37 °C. The cells were washed again and subsequently incubated with an anti-MUC2 primary antibody (1:800) at 37 °C, followed by an Alexa Fluor 594-conjugated secondary antibody (1:200) at 37 °C. For single occludin staining, the sections were incubated with an anti-occludin primary antibody (1:100) at 37 °C, followed by incubation with an Alexa Fluor 594-conjugated secondary antibody (1:200) at 37 °C. PBS washes were performed after each antibody incubation step. Finally, the nuclei were counterstained with DAPI at room temperature. The sections were thoroughly rinsed with tap water and mounted using an

anti-fade mounting medium.

2.8 Blood biochemical and endotoxin measurements

Serum biomarkers of systemic inflammation, oxidative status, and endotoxin levels were evaluated. Commercial sandwich enzyme-linked immunosorbent assay (ELISA) kits were used to quantify serum IL-6, IL-10, IL-17A, TNF-α-, IL-1β, SOD, GSH-Px, and MDA levels. Serum endotoxin levels were determined independently using a quantitative LPS detection kit.

2.9 Metabolomic profiling and network-based target analysis of pasteurized fermented milk

A 100 μL aliquot of each pasteurized fermented milk sample was combined with 400 μL of extraction solvent consisting of methanol and acetonitrile (1:1, v/v) containing an isotope-labeled internal-standard mixture. After vortex mixing for 30 s, the samples were sonicated in an ultrasonic bath maintained at 4 °C for 30 min and incubated at −20 °C for 30 min. The samples were centrifuged at 13,000 rpm for 15 min at 4 °C, and the supernatants were passed through a 0.22 μm membrane filter. The filtered extracts were analyzed using a UHPLC-Orbitrap Exploris 240 high-resolution mass spectrometer. Chromatographic separation was achieved using an ACQUITY UPLC HSS T3 column (2.1 × 100 mm, 1.8 μm; Waters, Milford, MA, USA). Mass spectra were acquired in positive- and negative-ion modes over an m/z range of 70–1050. Raw data were processed using Progenesis QI software (Waters Corporation, Milford, MA, USA) for peak detection, extraction, alignment, and integration. Putative metabolite annotation was performed using HMDB (http://www.hmdb.ca/), Metlin (https://metlin.scripps.edu/), and the Majorbio in-house database. Features with missing observations in >20% of the samples in any group were excluded. The remaining missing values were imputed using the minimum observed value, after which total-sum normalization was applied. Variables with QC-RSD >30% were removed, and $\log_{10}$ transformation was applied to obtain the final data matrix.

SMILES identifiers for the annotated metabolites were retrieved from PubChem (https://pubchem.ncbi.nlm.nih.gov/). The potential targets of these metabolites were predicted using Swiss Target Prediction (http://swisstargetprediction.ch/). Targets associated with IBD were compiled from GeneCards (https://www.genecards.org/) and OMIM (https://www.omim.org/), after which the targets shared by the metabolite- and disease-associated datasets were retained for subsequent analyses. Pathway enrichment analysis was conducted using DAVID (https://davidbioinformatics.nih.gov/), whereas protein–protein interaction (PPI) analysis was performed using STRING (https://string-db.org/). Cytoscape was used to construct compound-target-pathway interaction networks illustrating the relationships among candidate metabolites, shared targets, and enriched pathways[26].

2.10 Fecal metagenomic sequencing and data processing

Genomic DNA was isolated from fecal samples using a Tiangen magnetic bead extraction kit. For each sample, 1 μg of genomic DNA meeting the specified quality criteria was used to construct a sequencing library using the NEBNext® Ultra DNA Library Prep Kit for Illumina. DNA was randomly fragmented to approximately 350 bp using a Covaris ultrasonicator. Library preparation subsequently comprised end repair, A-tailing, adapter ligation, purification, and PCR amplification. The library concentration and fragment size distribution were evaluated using a Qubit 2.0 fluorometer and Agilent 2100 bioanalyzer, respectively. Libraries that satisfied the quality control (QC) criteria were sequenced on an Illumina NovaSeq 6000 platform to generate paired-end reads. Raw sequencing reads were filtered to eliminate low-quality and contaminating sequences. High-quality reads were aligned against the host reference genome using bowtie2[27] with default parameters, and host-derived sequences were removed. Microbial taxonomic profiles and functional pathway abundance were generated using MetaPhlan4 [28] and HUMAnN3[29], respectively.

2.11 Fecal untargeted metabolomics detection and data processing

A weighed aliquot of each fecal sample was combined with 600 μL of methanol containing 2-chloro-L-phenylalanine. The samples were vortex-mixed for 30 s, homogenized with steel beads for 120 s, and sonicated at room temperature for 10 min. Following centrifugation at 12,000 × g for 10 min at 4 °C, the supernatant was passed through a 0.22 μm membrane filter. Chromatographic separation was performed using a Thermo Scientific Ultimate 3000 UHPLC system equipped with an ACQUITY UPLC HSS T3 column (2.1 × 100 mm, 1.8 μm; Waters, Milford, MA, USA). The eluates were analyzed using a Thermo Scientific Q Exactive Focus mass spectrometer equipped with an electrospray ionization source. Data were acquired in separate positive- and negative-ionization modes, with both MS1 and MS2 spectra collected. Raw mass-spectrometry files were converted to mzXML format using MSConvert within the Proteowizard software package (version 3.0.8789) [30]. Peak detection, filtering, and alignment[31] were performed in R using the XCMS package to produce a quantitative feature-intensity matrix. QC-based signal correction was subsequently applied to minimize the systematic analytical variations. Features with a coefficient of variance below 30%[32] across QC samples were retained for downstream analysis. Compound identification was performed by matching the detected features against public metabolite and spectral databases, including HMDB, MassBank, LipidMaps, mzCloud, KEGG, and Nomics in-house library. A mass error threshold of <15 ppm was applied during database matching.

2.12 Determination of short-chain fatty acids

Fecal SCFAs were quantified using a Thermo Scientific Trace 1300 gas chromatograph coupled to a TSQ 9000 mass spectrometer. Calibration standards were prepared in a water/diethyl ether matrix containing 4-methylvaleric acid (375 μg/mL) as the internal standard. For sample preparation, each fecal sample was combined with 500 μL of water and glass beads,

homogenized, and centrifuged at 12,000 rpm for 10 min at 4 °C. A 200 μL aliquot of the resulting aqueous supernatant was sequentially combined with 100 μL of 15% phosphoric acid, 20 μL of an internal standard, and 280 μL of diethyl ether. Following a second centrifugation under identical conditions, the supernatant was collected for analysis. Chromatographic separation was achieved using an Agilent HP-INNOWAX capillary column (30 m × 0.25 mm × 0.25 μm). A 1 μL aliquot was introduced in split-injection mode at a split ratio of 10:1. Helium was used as the carrier gas at a flow rate of 1.0 mL/min. The initial oven temperature was set to 90 °C and subsequently increased to 120 °C at 10 °C/min, 150 °C at 5 °C/min, and finally to 250 °C at 25 °C/min. The final temperature was maintained for 2 min. The mass spectrometric conditions comprised an electron impact (EI) ion source temperature of 300 °C, a transfer line temperature of 250 °C, and an electron energy of 70 eV. Data were acquired in the selected-ion monitoring (SIM) mode[33-35].

2.13 Quantification of fecal tryptophan

Fecal tryptophan levels were quantified using ultra-high-performance liquid chromatography–tandem mass spectrometry (UPLC-MS/MS). A tryptophan standard was dissolved in 50% methanol, serially diluted with 10% methanol to generate calibration solutions, and stored at −20 °C. For sample preparation, an aliquot of each fecal sample was combined with 80% methanol and steel beads, mechanically homogenized, and diluted with a 10% methanol solution. Following centrifugation at 12,000 rpm for 5 min at 4 °C, the resulting supernatant was further diluted with 10% methanol and supplemented with a Trp-d3 internal standard (10 ppb) before injection. Chromatographic separation was achieved using an ACQUITY UPLC® HSS T3 column maintained at 40 °C, with a mobile phase flow rate of 0.3 mL/min. Mobile phase A comprised water containing 0.1% formic acid, and mobile phase B comprised methanol with 0.1% formic acid. The analytes were resolved using gradient elution. Tandem mass spectrometric detection was performed in the positive electrospray ionization mode with a source temperature of 500 °C, an ion-spray voltage of 5500 V, and data acquisition via multiple-reaction monitoring (MRM)[36,37].

2.14 Colonic transcriptome sequencing and data processing

Total RNA was extracted and purified from the colon tissue samples using TRIzol reagent. RNA concentration and purity were evaluated using a NanoDrop ND-1000 spectrophotometer, whereas RNA integrity was assessed using a 2100 Bioanalyzer and agarose gel electrophoresis. Polyadenylated (poly(A)) mRNA was enriched from total RNA using oligo(dT) magnetic beads and subsequently fragmented. Sequencing libraries were prepared through reverse transcription, second-strand cDNA synthesis, double-stranded DNA end repair, and A-tailing. The resulting libraries were sequenced as 150-bp paired-end reads (PE150) on an Illumina NovaSeq™ 6000 platform, according to the standard protocol. Raw reads were processed for QC using fastp (https://github.com/OpenGene/fastp) to remove adapter sequences, duplicate reads, and

low-quality reads. The retained high-quality reads were mapped to the mouse reference genome (GRCm38) using HISAT2 (https://ccb.jhu.edu/software/hisat2). Transcripts were assembled, and gene and transcript abundances were quantified using StringTie (https://ccb.jhu.edu/software/stringtie), with expression levels reported as FPKM. Between-group differential gene expression was evaluated using the R package edgeR. Differentially expressed genes were subjected to KEGG pathway enrichment analysis using DAVID (https://david.ncifcrf.gov/).

2.15 Statistical analysis

Statistical analyses of general experimental indices, gut microbial features, targeted metabolite concentrations, differentially expressed genes, and pathway-enrichment results were conducted using R (version 4.5.1). Gut microbial metabolic pathways were compared among groups using the Kruskal-Wallis test. For all remaining parameters, between-group differences were evaluated using either the non-parametric Wilcoxon rank-sum test or t-test, as appropriate. Microbial α-diversity indices, principal coordinates analysis (PCoA) based on Bray-Curtis dissimilarities, and analysis of similarities (ANOSIM) were computed and visualized using the R packages *Vegan* and *Ggpubr*. Untargeted fecal metabolomics data were analyzed using MetaboAnalyst (https://www.metaboanalyst.ca) to identify differentially abundant metabolites and enriched metabolic pathways. Associations between microbial taxa and metabolites were evaluated using Spearman rank-correlation coefficients, whereas relationships between general experimental indices and microbial taxa or metabolites were assessed using Pearson product–moment correlation coefficients. Correlation magnitudes were categorized as weak when $0.3 < |r| \leq 0.6$, moderate when $0.6 < |r| \leq 0.8$, and strong when $|r| > 0.8$. Metabolites and genes were classified as differentially abundant and differentially expressed, respectively, when the fold change (FC) > 1.5 or FC < 0.67 and $P < 0.05$. A p-value of < 0.05 was considered statistically significant, while $P > 0.05$ indicated no significant difference between groups.

3.Result

3.1 Probiotic fermentation enhanced the metabolic profile of pasteurized fermented milk

Untargeted metabolomic analysis identified marked differences between pasteurized fermented milk without probiotic supplementation and the three pasteurized probiotic-fermented milk formulations. Principal component analysis (PCA) revealed distinct separation among the four formulations (Fig. 1A; $R = 1$, $P = 0.001$), indicating substantial differences in metabolite profiles. Compared with the PRE formulation, the Probio-M8, PC-01, and PM8 formulations contained 53, 57, and 61 significantly downregulated metabolites, respectively, and 32, 9, and 30 significantly upregulated metabolites, respectively (Fig. 1B–D; $P < 0.05$).

The upregulated differential metabolites primarily comprised organic acids, lipids, and lipid-like molecules (Fig. 1E–G).

To assess the potential therapeutic relevance of these formulations for IBD, the predicted targets of the differential metabolites were compared with genes associated with colitis, UC, CD, and IBD. This analysis identified 296, 189, and 273 shared targets for the Probio-M8, PC-01, and PM8 formulations, respectively (Fig. 1H). These targets were enriched in inflammation-related biological processes, including immune responses and responses to LPS (Fig. 1I). Collectively, these findings suggest that the three pasteurized probiotic fermented milk formulations may alleviate IBD by modulating inflammation- and immunity-associated pathways.

3.2 Pasteurized probiotic fermented milk attenuates DSS-induced IBD in mice

Chronic colitis was induced in C57BL/6J mice through cyclic administration of 2.5% DSS to evaluate the protective effects of the four pasteurized fermented milk formulations (Fig. 2A). Compared with the NC group, the DSS group exhibited an elevated DAI and a significantly reduced colon length-to-weight ratio. Compared with the DSS group, all pasteurized fermented milk formulations reduced the DAI score to varying degrees and significantly restored the colon length-to-weight ratio (Fig. 2B–D, $P < 0.05$).. Notably, the colon length-to-weight ratio in the PM8 group recovered to a level comparable with that in the NC group ($P > 0.05$), indicating that the PM8 formulation exerted the strongest protective effect against DSS-induced colon shortening and edema. Moreover, Probio-M8 and PM8 formulations significantly ameliorated colonic tissue damage in DSS-treated mice (Fig. 2D-E,$P < 0.05$). The PRE and PC-01 formulations also produced modest improvements; however, these effects were not statistically significant ($P > 0.05$).

3.3 Pasteurized probiotic fermented milk alleviates intestinal barrier damage, inflammation, and oxidative stress

DSS administration caused substantial intestinal barrier disruption and systemic inflammation, as demonstrated by the markedly reduced expression of the epithelial tight junction proteins ZO-1 and occludin and the mucin protein MUC2, along with significantly elevated serum LPS levels (Fig. 2G–I; $P < 0.05$). Serum concentrations of the pro-inflammatory cytokines IL-17A, IL-6, IL-1β, and TNF-α were also significantly increased, whereas the concentration of the anti-inflammatory cytokine IL-10 was significantly decreased (Fig. 2J; $P < 0.05$). In addition, DSS treatment severely disrupted redox homeostasis, as indicated by a significant increase in MDA content and marked reductions in antioxidant enzyme (GSH-PX and SOD) levels (Fig. 2K, $P < 0.05$).

Compared with the DSS group, all pasteurized fermented milk formulations significantly increased occludin expression in colonic tissues and reduced serum LPS levels ($P < 0.05$).

Colonic MUC2 expression was significantly increased in the PC-01 group ($P < 0.05$), ZO-1 expression was markedly elevated in the M8 group ($P < 0.05$). These findings indicate that the formulations improve colonic barrier integrity through distinct regulatory patterns. Compared with the PRE group, colonic ZO-1 expression was significantly higher in the M8 group ($P < 0.05$), whereas occludin expression was significantly higher in the PM8 group ($P < 0.05$). The PM8 group exhibited a significant reduction in serum LPSlevels ($P < 0.05$). These results suggest that Probio-M8 and PM8 formulations were more effective than the PRE formulation in restoring intestinal barrier function in DSS-treated mice, although their effects appeared strain-dependent.

Compared with the DSS group, all pasteurized probiotic fermented milk formulations significantly reduced the serum concentrations of the pro-inflammatory cytokines IL-6, IL-1β, and TNF-α and increased the concentration of the anti-inflammatory cytokine IL-10 ($P < 0.05$). Notably, TNF-α and IL-10 levels in the PM8 group returned to values comparable to those in the NC group ($P > 0.05$). Compared with the PRE group, the PC-01 formulation significantly reduced IL-6 levels, whereas the PM8 formulation significantly reduced TNF-α levels and increased IL-10 levels ($P < 0.05$). These results demonstrate that the fermented milk formulations differentially regulated inflammatory cytokines, with PC-01 and PM8 formulations producing stronger anti-inflammatory effects than the PRE formulation.

Regarding oxidative stress, the pasteurized probiotic fermented milk formulations significantly increased SOD and GSH-PX levels and reduced MDA content compared with the DSS group. In contrast, the PRE formulation did not produce significant changes in these parameters ($P > 0.05$). Furthermore, the Probio-M8 and PM8 formulations increased GSH-PX levels more effectively than the PC-01 formulation. The Probio-M8 formulation also significantly reduced MDA content compared to the other fermented milk formulations ($P< 0.05$), restoring it to a level comparable to that in the NC group ($P > 0.05$). Collectively, these findings indicate that the pasteurized probiotic fermented milk formulations alleviated oxidative stress to varying degrees and were more effective than the PRE formulation.

3.4 Pasteurized probiotic fermented milk restores DSS-induced gut microbiota dysbiosis

To investigate how pasteurized probiotic fermented milk modulates the gut microbiota of DSS-treated mice, we compared the intestinal microbial diversity and community structure across the experimental groups (Fig. 3). No significant differences in α-diversity indices (Shannon and Simpson indices) were observed between or within the groups (Fig. 3A–B). We then performed PCoA combined with ANOSIM to assess the changes in the microbial community structure (Fig. 3C–G). This analysis revealed a significant separation between the M8 and DSS groups ($P < 0.01$; Fig. 3E) and a marginally significant separation between the PM8 and DSS groups ($P = 0.09$; Fig. 3G). No significant separation was observed between any

other group pairs ($P > 0.05$).

We further analyzed the data at the species level to identify bacterial taxa that changed over the experimental period and clarify which bacteria were involved in ameliorating IBD-related symptoms after treatment. The results showed that after DSS treatment, the abundance of beneficial bacteria, such as *Enterococcus hirae*, *Paramuribaculum intestinale*, and *Muribaculum intestinale*, decreased, whereas that of opportunistic pathogens, such as *Parasutterella excrementihominis* increased. Following treatment with different pasteurized fermented milk products, the gut microbiota of DSS-treated mice exhibited various degrees of recovery. Compared with the DSS group, all pasteurized fermented milk products consistently restored the abundance of *Parasutterella excrementihominis* and *Enterococcus hirae*. In addition, Probio-M8 formulations restored the relative abundance of *Muribaculum intestinale*; PC-01 formulations restored *Paramuribaculum intestinale*; and the combined PM8 formulations restored both *Paramuribaculum intestinale* and *Muribaculum intestinale* (Fig. 3H).

We then examined whether these changes in microbiota composition were accompanied by alterations in functional pathways. HUMAnN3 was used to annotate the functional profiles of the microbial communities in each group. We selected differential metabolic pathways with $P < 0.004$ for clustering analysis to reveal distinct response patterns of gut microbial metabolism to pasteurized fermented milk treatment. Specifically, compared with the NC group, the DSS group exhibited reduced expression of pathways within clusters 1 and 5, including those involved in amino acid biosynthesis, the superpathway of coenzyme A biosynthesis III (mammalian), and nucleotide biosynthesis. Probio-M8 formulations increased the expression of pathways such as L-cysteine biosynthesis VI (from L-methionine), coenzyme A biosynthesis III (mammalian), and L-histidine biosynthesis. Similarly, PC-01 formulations enhanced pathways, including S-adenosyl-L-methionine salvage I and CMP pseudominate biosynthesis. Furthermore, the combined PM8 formulations increased the expression of pathways including the superpathway of coenzyme A biosynthesis III (mammalian), L-histidine biosynthesis, and S-adenosyl-L-methionine salvage I. Notably, a trend heatmap showed that the three probiotic-containing pasteurized fermented milk products were more effective than the pasteurized fermented milk without probiotic addition in modulating these pathways within the examined clusters (Fig. 3I).

3.5 Pasteurized probiotic fermented milk restores fecal metabolite concentrations in DSS-treated mice

Untargeted metabolomics analysis was conducted to investigate changes in fecal metabolite profiles following pasteurized fermented milk treatment. PCA showed that the QC

samples were tightly clustered, indicating good reproducibility and high instrument stability (Fig. 4A), thereby ensuring the accuracy of our experimental results. We then identified differential metabolites between groups based on fold change and p-values. The results showed that DSS treatment led to the upregulation of 191 metabolites and downregulation of 882 metabolites. Compared with the DSS group, the PRE, M8, PC-01, and PM8 groups exhibited 78, 128, 102, and 100 upregulated metabolites and 121, 93, 214, and 112 downregulated metabolites, respectively (Fig. 4B–F, $P < 0.05$).

Annotation of the differential metabolites revealed that after DSS treatment, the levels of compounds such as bisphenol A and PGD_2 ethanolamide increased. After intervention with Probio-M8 formulations, the levels of l-fucose-, α-tocotrienol-, and taxifolin significantly increased ($P < 0.05$). After PC-01 formulations treatment, the levels of pyridoxine and loliolide significantly increased ($P < 0.05$). Similarly, after treatment with the combined PM8 formulations, the levels of hippuric acid, zearalenone, and captopril significantly increased ($P < 0.05$). In contrast, PRE formulations only increased the levels of a small number of metabolites (Fig. 4G). Pathway enrichment analysis revealed that the differential metabolites were predominantly involved in vitamin B_6 metabolism, pyrimidine metabolism, purine metabolism, and tyrosine metabolism (Fig. 4H).

Procrustes analysis revealed a concordance between the gut microbiota and potentially active metabolites (Fig. 4I; $r = 0.348$, $P = 0.012$), highlighting the association between the gut microbiome and metabolome. Spearman correlation analysis was performed to explore the relationships between fecal microbial taxa and differential metabolites. The results indicated that *Parasutterella excrementihominis* was negatively correlated with pyridoxine, zearalenone, and taxifolin ($P < 0.05$). *Enterococcus hirae* was positively correlated with calgam and 2-methoxyadenosine. *Heminiphilus faecis* was positively correlated with neomycin and captopril, and *Muribaculum intestinale* was positively correlated with L-fucose, taxifolin, and calgam ($P< 0.05$) (Fig. 4J).

3.6 Pasteurized probiotic fermented milk increases fecal short-chain fatty acid and tryptophan concentrations in DSS-treated mice

SCFAs and tryptophan metabolism are crucial for maintaining intestinal homeostasis, and inflammatory conditions can disrupt this balance. Therefore, we quantified fecal levels of SCFAs and tryptophan metabolites. In DSS-treated mice, the fecal concentrations of acetic and butyric acids were significantly lower than those in the controls ($P < 0.05$). Compared with DSS treatment alone, mice receiving pasteurized probiotic-fermented milk from Probio M8 or PM8 exhibited significantly higher fecal butyric acid concentrations, whereas mice administered pasteurized fermented milk showed a significant increase in fecal acetic acid (Fig. 4K–L, $P< 0.05$).

After DSS treatment, fecal levels of kynurenic acid (KYNA), 3-hydroxyanthranilic acid (3-HAA), and cinnabarinic acid were significantly decreased ($P < 0.05$). Compared with the DSS group, pasteurized probiotic-fermented milk from Probio-M8 significantly increased fecal 3-HAA and cinnabarinic acid levels ($P < 0.05$). Pasteurized probiotic fermented milk from PC-01 significantly increased 3-HAA and KYNA levels ($P < 0.05$). Similarly, pasteurized probiotic-fermented milk from PM8 significantly elevated 3-HAA and cinnabarinic acid levels ($P < 0.05$). In contrast, PRE increased only KYNA levels ($P < 0.05$) without significantly affecting other tryptophan metabolites ($P > 0.05$) (Fig. 4M–O).

3.7 Pasteurized probiotic fermented milk alters the colonic transcriptomic profile of DSS-induced colitis mice

To investigate the effects of pasteurized probiotic-fermented milk on gene expression and related molecular mechanisms in the colonic tissues of mice with chronic inflammation, we conducted transcriptomic analysis. Compared with the NC group, DSS treatment significantly altered gene expression, resulting in 613 upregulated and 2, 640 downregulated genes. Compared with the DSS group, administration of pasteurized fermented milk from PRE, Probio-M8, PC-01, and PM8 significantly upregulated 397, 129, 713, and 67 genes, respectively. These treatments also significantly downregulated 87, 47, 443, and 126 genes (Fig. 5A, $P< 0.05$). We then annotated the differentially expressed genes using the KEGG pathway analysis. Compared to the NC group, DSS induction upregulated pathways related to IL-17 signaling, TNF signaling, Th17 cell differentiation and IBD. Conversely, it downregulated pathways including PPAR signaling, serotonergic synapse, gap junction, TGF-β signaling,, tight junction, and AMPK signaling, as well as pathways associated with digestion, absorption, amino acid synthesis, and metabolism. After treatment with PRE formulations, pathways such as starch and sucrose metabolism, endocrine and other factor-regulated calcium reabsorption, and protein digestion and absorption were upregulated. Administration of Probio-M8 formulations upregulated the PPAR and AMPK signaling pathways, serotonergic synapse, retinol metabolism, and pathways related to digestion and absorption. Similarly, treatment with PC-01 formulations upregulated the PPAR and AMPK signaling pathways, tight junctions, FoxO signaling pathway, adherens junction, and pathways related to digestion and absorption. In contrast, administration of PM8 formulations downregulated the IL-17 signaling pathway, TNF signaling pathway, Th17 cell differentiation, and IBD pathway (Fig. 5B–F, $P < 0.05$).

3.8 Correlations of signature gut microbiota and metabolites with basic parameters

Pearson correlation analysis indicated that *Parasutterella excrementihominis* was positively associated with DAI, IL-6, IL-1β, TNF-α, MDA, and LPS and negatively associated with occludin, SOD, and GSH-Px. Among the SCFAs, acetic acid displayed negative correlations with DAI, HE score, IL-6, IL-1β, IL-17A, TNF-α, MDA, and LPS, and positive correlations with IL-10, SOD, and GSH-Px. In contrast, butyric acid was negatively correlated

with DAI and IL-17A and positively correlated with occludin. The tryptophan metabolites 3-HAA and cinnabarinic acid were negatively correlated with DAI, IL-6, IL-1β, IL-17A, TNF-α, MDA, and LPS. These metabolites were positively correlated with IL-10, SOD, and GSH-Px. KYNA was negatively correlated with IL-6, IL-1β, IL-17A, TNF-α, and LPS, and positively correlated with occludin (Fig. 5G).

4. Discussion

In this study, we evaluated the effects of pasteurized fermented milk supplemented with various probiotics (*Bifidobacterium animalis* subsp. *Lactis* Probio-M8, *Lactobacillus paracasei* PC-01, and their combination) on intestinal inflammatory diseases and examined their alleviating effects and underlying mechanisms in a DSS-induced mouse modelof IBD. The core findings indicate that pasteurized probiotic-fermented milk is enriched with bioactive compounds capable of modulating immune responses. Network pharmacology analysis revealed that the metabolites of this fermented milk are enriched in inflammation-related pathways. Moreover, probiotic supplementation enhanced the therapeutic efficacy of the base fermented milk in DSS-induced IBD mice, particularly improving intestinal barrier repair, antioxidant defenses, and the restoration of key gut microbiota and metabolite profiles. These results address the central question by demonstrating that probiotic supplementation enhances the therapeutic effects of pasteurized fermented milk on IBD by restoring gut microecology and metabolic profiles.

Metabolic profiling of pasteurized probiotic-fermented milk revealed that fermentation increased the levels of metabolites, such as organic acids, lipids, and phenylpropanoids, which are known for their nutritional and bioactive properties. Organic acids serve as energy substrates, exert anti-inflammatory and antioxidant effects, modulate gut microbiota composition and function, thereby contributing to host intestinal homeostasis[38,39]. These acids can improve transepithelial electrical resistance (TEER) and increase the expression of tight junction proteins, effectively alleviating damage to intestinal epithelial cells under inflammatory conditions[40]. Additionally, this mixture of organic acids can enhance intestinal barrier function by upregulating tight junction proteins, such as occludin and ZO-1, while reducing the production of pro-inflammatory cytokines IL-6 and TNF-α[41]. Dietary supplementation with organic acids can also alleviate LPS-induced intestinal barrier damage by inhibiting the activation of the TLR4/NF-κB signaling pathway, thereby reducing LPS translocation into the circulation and systemic inflammation[42,43]. Lipids and phenylpropanoids are natural bioactive compounds that modulate intestinal inflammation[44]. Network pharmacology predictions indicated that PPARs/PXR are the key regulators of lipid metabolism. Signaling through these receptors inhibits the release of inflammatory mediators (such as IL-1β and TNF-α) by antagonizing NF-κB transcriptional activity while maintaining epithelial barrier integrity. Conversely, phenylpropanoids promote IL-10 secretion and regulatory T cell (Treg)

differentiation via the AHR pathway, thereby reshaping the intestinal immune microenvironment[45]. This mechanism was experimentally validated. Zhang et al. demonstrated that phenylpropanoids isolated from Chinese olive significantly inhibited LPS-induced nitric oxide (NO) production and ROS accumulation, exhibiting potent anti-inflammatory and antioxidant activities[44]. Based on these findings, this study employed network pharmacology to explore the associations between these metabolites and IBD. The analysis showed that targets corresponding to metabolites upregulated by probiotic fermentation were enriched in pathways related to "inflammatory response" and "response to lipopolysaccharide" when they overlapped with disease targets. From these predictions, all three pasteurized probiotic fermented milk formulations exert broad protective effects by modulating the host immune response to LPS and suppressing the overactivated inflammatory cascade, thereby alleviating intestinal inflammation and repairing the damaged barriers.

Given the potential application of pasteurized probiotic fermented milk in alleviating IBD, we evaluated its effects in a DSS-induced IBD mouse model of colitis. The results showed that pasteurized fermented milk reduced the DAI score and increased the colon length-to-weight ratio. Elevated DAI, colon shortening, and edema are typical features of DSS-induced colitis, and previous studies have confirmed that probiotic-fermented milk can effectively ameliorate such lesions[14,46]. However, studies on the effects of pasteurized fermented milk in this context are scarce. We speculate that these ameliorative effects may be closely related to the beneficial metabolites and residual bacterial components produced during fermentation. Probiotics can convert milk macronutrients into various bioactive metabolites during fermentation. These metabolites participate in intestinal epithelial energy metabolism, regulate immune responses, and maintain mucosal barrier function, as suggested by network pharmacology enrichment analysis. In contrast, bacterial components retained after pasteurization (such as peptidoglycan and lipoteichoic acid) also possess immunomodulatory activities. For example, peptidoglycan from *Bifidobacterium adolescentis* can induce regulatory B cells to secrete IL-10, thereby alleviating intestinal inflammation. Similarly, *Lactobacillus*-derived lipoteichoic acid can mitigate inflammatory responses in colitis mice[47-49]. Therefore, even though probiotics are no longer viable, their fermentation products and bacterial components can still exert protective effects on the intestine. This mechanism likely underlies the observed ameliorative effects of pasteurized fermented milk on IBD. Furthermore, pasteurized fermented milk containing both Probio-M8 and PM8 significantly reduced pathological damage scores, whereas the formulation containing only PC-01 showed a trend toward improvement but did not reach statistical significance. We speculate that this difference may be attributable to strain-specific- characteristics that were not fully manifested at the pathological phenotype level.

Furthermore, because correcting inflammatory dysregulation is a central therapeutic objective in IBD, biological agents that inhibit IL-6 or TNF-αmediated signaling have been

clinically used to control intestinal inflammation[50,51]. IL-10 is a pivotal immunoregulatory cytokine that is required for intestinal immune homeostasis. Its deficiency can accelerate IBD progression by permitting microbiota-driven hyperactivation of immune responses; therefore, strategies that restore IL-10 activity may complement anti-TNF therapy. Accordingly, IL-10-knockout mice are widely used as a classical experimental model of IBD[52,53]. In the present study, pasteurized probiotic fermented milk suppressed the elevated levels of the pro-inflammatory cytokines IL-6, IL-1β, and TNF-α while significantly increasing the anti-inflammatory cytokine IL-10. These coordinated changes indicate that the intervention rebalanced pro- and anti-inflammatory signaling and may therefore have value as an adjunctive strategy for IBD management.

Mucosal barrier dysfunction and intestinal inflammation are closely interconnected features of IBD. Excessive concentrations of pro-inflammatory cytokines, including IL-6, IL-1β, and TNF-α, can disrupt mucosal architecture, reduce tight-junction protein expression, and consequently impair intestinal barrier integrity[54-56]. For example, Rawat et al. demonstrated that co-incubation of Caco-2 cell monolayers with IL-1β increased tight junction permeability and concurrently decreased occludin protein abundance[57].Consistent with this mechanism, the attenuation of inflammation observed in the present study coincided with increased occludin expression and reduced serum LPS concentrations following the administration of pasteurized fermented milk. Occludin is an essential structural component of epithelial tight junctions that contributes substantially to the maintenance of barrier integrity[58]. Conversely, serum LPS is commonly regarded as an indicator of intestinal barrier disruption. Under physiological conditions, an intact intestinal epithelium restricts the translocation of LPS. However, when barrier integrity is compromised, LPS can enter the circulation and promote chronic low-grade inflammation, thereby aggravating IBD progression[59-61]. However, barrier-related responses differed among strain-specific fermented milk treatments. Pasteurized probiotic-fermented milk produced with Probio-M8 additionally increased ZO-1 protein expression. ZO-1, the first TJ-associated protein identified, functions as a central scaffolding molecule that connects occludin and other transmembrane junctional proteins to the cytoskeleton through multiple interaction domains. Therefore, it stabilizes the tight junction architecture and supports epithelial barrier function[62]. In contrast, pasteurized probiotic-fermented milk produced with PC-01 significantly increased MUC2 expression. MUC2 is the principal structural component of the intestinal mucus layer and protects the intestinal epithelium against mechanical injury and pathogen invasion[63,64]. Collectively, these findings suggest that pasteurized probiotic-fermented milk may alleviate colitis through complementary mechanisms, including suppression of excessive inflammatory signaling, restoration of tight-junction organization, and reinforcement of the intestinal mucus barrier. Oxidative stress provides an additional mechanistic link between intestinal inflammation and barrier dysfunction. Pro-inflammatory cytokines stimulate excessive ROS production in intestinal epithelial cells, resulting in barrier

disruption, DNA fragmentation, and cell death. Dysregulated necrotic death of epithelial cells can further amplify pro-inflammatory immune responses, creating a self-perpetuating cycle of inflammation and oxidative damage[65]. The host counteracts this process through an integrated antioxidant defense system comprising non-enzymatic antioxidants, including GSH, and antioxidant enzymes, such as SOD and GSH-PX. SOD catalyzes the conversion of superoxide radicals into molecular oxygen and hydrogen peroxide, whereas GSH-PX reduces hydrogen peroxide to water[66]. MDA is widely used as a biomarker for oxidative damage[67]. In the present study, DSS exposure induced a characteristic oxidative stress phenotype, as evidenced by diminished SOD and GSH-PX concentration and pronounced MDA accumulation. Intervention with pasteurized probiotic-fermented milk significantly reversed these alterations. In contrast, PRE pasteurized fermented milk showed little improvement in oxidative stress indices. This divergence suggests that the probiotics used during fermentation substantially contributed to the antioxidant activity of the pasteurized products. These products may strengthen endogenous antioxidant defenses, limit oxidative injury, and potentially disrupt the inflammation–oxidative stress cycle underlying colitis progression.

To further elucidate the underlying mechanisms, we observed that restoration of the gut microbiota is a key mediator of the protective effects of pasteurized probiotic fermented milk. All tested pasteurized fermented milk products partially reversed DSS-induced microbial dysbiosis. Notably, they suppressed the potential pathogen *Parasutterella excrementihominis*, which is highly enriched in the feces of patients with active UC and can exacerbate experimental colitis and colitis-associated carcinogenesis (CAC) through its metabolites. Additionally, clinical studies have found that the genus *Parasutterella* is closely associated with obesity, diabetes, and IBD (particularly during active phases)[7,68]. This genus can interfere with tryptophan metabolic pathways, affecting the levels of key metabolites, such as KYNA[69]. Further analysis indicated that *P. excrementihominis* abundance was positively correlated with DAI scores and pro-inflammatory cytokine levels. This finding confirms that this bacterium contributes to colitis progression as a potential pathogen. Pasteurized fermented milk also restored the abundance of beneficial bacteria, *Enterococcus hirae*. Through its ability to activate autophagy, *E. hirae* exhibits both anti-inflammatory and tissue-protective effects[70,71]. Deretic et al. further elucidated that autophagy plays a crucial regulatory role in maintaining homeostasis by simultaneously minimizing tissue damage and preserving effective immune defense[72]. Notably, pasteurized probiotic-fermented milk demonstrated unique benefits in modulating the gut microbiota, including the restoration of SCFA-producing bacteria, such as *Muribaculum intestinale* and *Paramuribaculum intestinale*. SCFAs are key energy sources and signaling molecules in colonic epithelial cells. They maintain intestinal homeostasis and enhance barrier function by promoting the expression of tight junction proteins[73]. *Muribaculum intestinale* converts succinate into SCFAs and is considered a beneficial member of the gut microbiota. *Paramuribaculum intestinale*, a representative species of the genus *Muribaculaceae*, produces

SCFAs and suppresses inflammatory microbiota[74]. This differential restoration of the microbiota led to significant changes in the functional metabolites. For example, pasteurized probiotic-fermented milk containing Probio-M8 or PM8 significantly increased butyric acid levels and restored the levels of immunomodulatory tryptophan metabolites, such as 3-HAA and cinnabarinic acid. In contrast, pasteurized probiotic-fermented milk containing the strain PC-01 restored the levels of another key tryptophan metabolite, KYNA. Previous studies have shown that butyric acid is a key bioactive metabolite that drives epithelial proliferation and provides energy to colonocytes. Its restoration is closely associated with an increased abundance of SCFA-producing bacteria[75]. The tryptophan metabolic pathway is a cornerstone of immune regulation, generating multiple bioactive compounds that play indispensable roles in quenching inflammation, fine-tuning the immune response, and maintaining neural functions[76]. Among these tryptophan-derived metabolites, 3-HAA inhibits the proliferation of Th1, CD8+ T, and natural killer (NK) cells. It also reduces the production of inflammatory cytokines and modulates the local oxidative status[77]. In both mice and humans, the severity of intestinal inflammation is negatively correlated with KYNA levels. Furthermore, KYNA supplementation can reduce colitis severity by activating the aryl hydrocarbon receptor (AhR) and remodeling cellular energy metabolism[78]. Our correlation analysis corroborated these findings.

Furthermore, pasteurized probiotic-fermented milk increased the levels of several fecal metabolites, including l-fucose-, taxifolin, pyridoxine, (–)-loliolide, and zearalenone etc. Specifically, L-fucose has been reported to attenuate DSS-induced oxidative stress, mitochondrial dysfunction, and apoptosis. It also ameliorates the peritoneal inflammatory microenvironment induced by a high-fat diet by reducing inflammatory-cell abundance and decreasing TNF-α, IL-6, and MCP-1 levels[79,80]. Similarly, taxifolin suppresses the expression of proinflammatory cytokines- and the phosphorylation of MAPK signaling components. In kidney injury models, taxifolin attenuates oxidative stress, inflammation, and apoptosis while restoring Nrf2 signaling[81,82]. Pyridoxine contributes substantially to amino acid metabolism, antioxidant defense, and the regulation of inflammatory cytokines. Previous studies have demonstrated that pyridoxine markedly reduces oxidative stress and restores antioxidant enzyme activities, thereby mitigating complications associated with a high-fat diet[83,84]. Moreover, (–)-loliolide effectively suppresses IFN-γ/TNF-α–induced oxidative stress and inflammatory responses by activating the Nrf2/HO-1 signaling pathway[85]. Zearalenone, albeit typically regarded as a mycotoxin has also been reported to increase the abundance of SCFA-producing gut microbial taxa and elevate fecal acetate concentrations in mice with colon cancer[86]. The correlation patterns among the gut microbiota, metabolites, and physiological parameters closely paralleled the phenotypic responses observed in mice. Integrated microbiota-metabolite analysis identified coordinated associations between changes in microbial taxa and metabolite profiles, providing insights into their potential interactions.

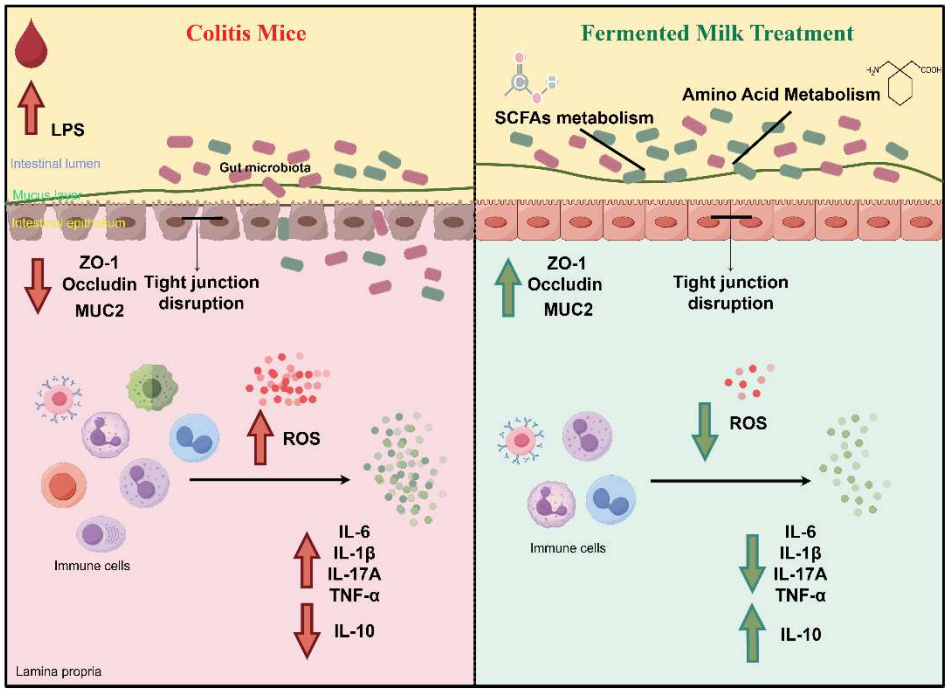
Probiotic supplementation partially restored the gut microbial structure by promoting beneficial bacteria and suppressing potentially harmful taxa. These compositional changes coincided with the reorganization of the host metabolite profile toward patterns associated with intestinal barrier repair, reduced inflammation, and enhanced antioxidant defense. Notably, PRE pasteurized fermented milk significantly increased acetic acid, KYNA, and several other metabolites, suggesting that this preparation retained some capacity to modulate the gut microbiota-metabolite axis despite the absence of added probiotics. This interpretation is consistent with its observed mitigation of IBD-related symptoms, regulation of inflammatory cytokines and intestinal barrier proteins, and partial restoration of gut microbial composition.

To further characterize the molecular mechanisms underlying these strain-dependent effects, we performed transcriptomic profiling. Pathway analysis revealed marked functional divergence between the treatments. Pasteurized probiotic-fermented milk produced with either Probio-M8 or PC-01 showed enrichment in the AMPK signaling pathway. Current evidence identifies AMPK is a central mediator of intestinal protection. Sun et al. reported that intestine-specific AMPK deletion exacerbated colitis, whereas pharmacological activation of AMPK with AICAR attenuated both acute and relapsing colitis[87]. These complementary loss- and gain-of function findings support the protective role of AMPK in the intestine. Accordingly, AMPK signaling may represent a shared molecular basis for the principal protective effects of Probio-M8 and PC-01. In addition to this common response, the two treatments displayed distinct pathway signatures. PC-01 treatment selectively enriched pathways associated with tight and adherens junctions. This transcriptomic signature closely aligned with the increased protein expression of occludin and MUC2 and preservation of intestinal barrier integrity. In contrast, Probio-M8 treatment preferentially affected pathways related to bioactive signaling and metabolism, including serotonergic synapses and retinol metabolism, suggesting a broader influence on local bioactive mediators. The PM8 combination treatment exhibited a different dominant mechanism. Rather than enriching AMPK signaling, it strongly suppressed classical pro-inflammatory pathways, including IL-17 and TNF signaling and Th17-cell differentiation. This molecular profile closely corresponds to the pronounced reductions in IL-17A and TNF-α levels, indicating that direct suppression of immune-inflammatory pathways may underlie its potent anti-inflammatory activity. The transcriptomic alterations induced by PRE pasteurized fermented milk, which contained no added probiotics, were concentrated primarily in pathways associated with nutrient digestion and absorption. No clear enrichment of anti-inflammatory or intestinal barrier-protective pathways was detected, which may explain the comparatively limited protection afforded by PRE against IBD. Notably, butyrate and tryptophan metabolites have been reported to exert dual roles: activating the AMPK pathway while directly suppressing the expression of pro-inflammatory cytokines such as IL-17A and TNF-α[88-91]. In line with the multi-omics findings, pasteurized probiotic-fermented milk alleviated colitis by restoring the abundance of key microbial taxa and elevating short-chain fatty acid and tryptophan metabolite

levels, thereby either activating the AMPK pathway or directly restraining inflammatory signaling cascades, depending on the specific formulation.

5.Conclusion

Our results show that pasteurized fermented milk can help restore gut microbial balance by suppressing the opportunistic pathogen *Parasutterella excrementihominis* and enriching *Enterococcus hirae*. This shift in the gut microbiota alters the fecal metabolome and partially restores gut microecological balance. Compared to pasteurized milk without probiotics, pasteurized probiotic-fermented milk further increased levels of SCFA-producing bacteria, including *Muribaculum_intestinale* and *Paramuribaculum_intestinale*. It also improved the levels of SCFAs (such as butyric acid) and tryptophan derivatives (such as 3-HAA and kynurenic acid) and significantly increased the concentrations of beneficial compounds with antioxidant and anti-inflammatory functions. These changes contributed to more pronounced reductions in inflammation, amelioration of intestinal barrier damage, and mitigation of oxidative stress. Transcriptomic analysis revealed distinct strain-specific effects. Fermented milk containing Probio-M8 preferentially activated AMPK-mediated metabolic processes. PC-01 milk also activated the AMPK pathway and specifically upregulated tight junction proteins, thereby strengthening the intestinal barrier. In contrast, the combined Probio-M8 and PC-01 milk exerted potent immunomodulatory effects, primarily by inhibiting key inflammatory pathways such as IL-17 and TNF signaling.



Author contributions

Lu Gao: Conceptualization, Methodology, Animal experiments, Data curation, Formal analysis, Writing - original draft.

Hongliang Li: Conceptualization, Data curation, Formal analysis.

Luping Yang: Validation, Resources.

Chang Yang: Validation, Resources.

Xinxue Zhao: Animal experiments, Resources.

Guohong Wang: Sample provision, Validation, Resources.

Xueli Li: Sample provision, Validation, Resources.

Meng Zhang: Validation, Resources.

Zhihong Sun: Methodology, Conceptualization, Supervision,. Funding acquisition.

Heping Zhang: Data curation, Writing - review & editing, Supervision, Funding acquisition.

Feiyan Zhao: Methodology, Conceptualization, Supervision, Resources.

Acknowledgements

We are profoundly thankful to Research Fund for the National Key R&D Program of China (2022YFD2100700,2024YFA1307002), the National Natural Science Foundation of China (32394053,U22A20540),Inner Mongolia Agricultural University High level/Excellent Doctoral Talent Introduction and Research Initiation Project (NDYB2023-24), and the earmarked fund for CARS36. Thanks for Figdraws.

Disclosures

The authors declare no competing interests.

Data availability

The metagenomic datasets generated and/or analysed during the current study are available in the National Genomics Data Center (NGDC, https://ngdc.cncb.ac.cn/) repository, accessible via the accession number CRA043874. The raw transcriptome sequencing data have been deposited in the NCBI Sequence Read Archive (SRA) under BioProject accession number PRJNA1510350 (https://www.ncbi.nlm.nih.gov/sra/PRJNA1510350).

References

1 Zhang, Z. *et al.* Baseline Gut Microbiome-Dependent Responses to Probiotic Treatments for IBD in Mice. *Engineering* (2026). https://doi.org/10.1016/j.eng.2025.02.025

2 Jin, Y., Madan, J., Radha B, K. & Anthony, B. P023 Identification of regulated mechanistic pathways and genes to protect intestinal barrier injury by larazotide acetate in an IBD microenvironment. *Journal of Crohn's and Colitis* (2020). https://doi.org/10.1093/ecco-jcc/jjz203.152

3 Mehandru, S. & Colombel, J.-F. The intestinal barrier, an arbitrator turned provocateur in IBD. *Nature Reviews Gastroenterology & Hepatology* (2020). https://doi.org/10.1038/s41575-020-00399-w

4 de Jesus, L. C. L. *et al.* Lactobacillus delbrueckii CIDCA 133 fermented milk modulates inflammation and gut microbiota to alleviate acute colitis. *Food Research International* (2024). https://doi.org/10.1016/j.foodres.2024.114322

5 Schreiber, S., Aden, K., Tran, F. & Rosenstiel, P. Rise of precision medicine: can it deliver on its promise in IBD? *Gut* (2025). https://doi.org/10.1136/gutjnl-2023-330000

6 Qiu, P. *et al.* The Gut Microbiota in Inflammatory Bowel Disease. *Frontiers in Cellular and Infection Microbiology* (2022). https://doi.org/10.3389/fcimb.2022.733992

7 Tan, H. *et al.* Parasutterella excrementihominis exacerbates experimental colitis and colitis-associated colorectal cancer via pathogenic NETosis activation. *Gut* (2026). https://doi.org/10.1136/gutjnl-2025-335887

8 Zhang, Z. *et al.* Regulatory role of short-chain fatty acids in inflammatory bowel disease. *Cell Communication and Signaling* (2022). https://doi.org/10.1186/s12964-022-00869-5

9 Zhao, H. *et al.* Short-chain fatty acid-producing bacterial strains attenuate experimental ulcerative colitis by promoting M2 macrophage polarization via JAK/STAT3/FOXO3 axis inactivation. *Journal of Translational Medicine* (2024). https://doi.org/10.1186/s12967-024-05122-w

10 Liu, Y.-J. *et al.* Parthenolide ameliorates colon inflammation through regulating Treg/Th17 balance in a gut microbiota-dependent manner. *Theranostics* (2020). https://doi.org/10.7150/thno.43716

11 Li, X.-J., Shan, Q.-Y., Wu, X., Miao, H. & Zhao, Y.-Y. Gut microbiota regulates oxidative stress and inflammation: a double-edged sword in renal fibrosis. *Cellular and Molecular Life Sciences* (2024). https://doi.org/10.1007/s00018-024-05532-5

12 Ma, S., Vidanarachchi, J. K. & Ranadheera, C. S. in *Probiotic Foods and Beverages : Technologies and Protocols* (eds Adriano Gomes da Cruz *et al.*) 1–33 (Springer US, 2023).

13 Cheng, S. *et al.* The probiotic fermented milk of Lacticaseibacillus paracasei JY062 and Lactobacillus gasseri JM1 alleviates constipation via improving gastrointestinal motility and gut microbiota. *Journal of Dairy Science* (2023). https://doi.org/10.3168/jds.2023-24154

14 Lao, L. *et al.* Anti-inflammation and gut microbiota regulation properties of fatty acids derived from fermented milk in mice with dextran sulfate sodium-induced colitis. *Journal of Dairy Science* (2022). https://doi.org/10.3168/jds.2022-21877

15 Mathur, H., Beresford, T. P. & Cotter, P. D. Health Benefits of Lactic Acid Bacteria (LAB) Fermentates. *Nutrients* (2020). https://doi.org/10.3390/nu12061679

16 Yoda, K. *et al.* Lactobacillus GG-fermented milk prevents DSS-induced colitis and regulates intestinal epithelial homeostasis through activation of epidermal growth factor receptor. *European Journal of Nutrition* (2013). https://doi.org/10.1007/s00394-013-0506-x

17 Zhao, J. *et al.* Improvement of sleep quality and sub-health conditions through pasteurized fermented milk consumption: A human intervention study. *Journal of Functional Foods* (2024). https://doi.org/10.1016/j.jff.2024.106562

18 Shi, J. *et al.* Preventive effects of Bifidobacterium lactis Probio-M8 on ovalbumin-induced food allergy in mice. *Food Science and Human Wellness* (2024). https://doi.org/10.26599/fshw.2022.9250250

19 Zhang, Z. *et al.* Bifidobacterium animalis Probio-M8 improves sarcopenia physical performance by mitigating creatine restrictions imposed by microbial metabolites. *npj Biofilms and Microbiomes* (2024). https://doi.org/10.1038/s41522-024-00618-1

20 Zhao, F. *et al.* Bifidobacterium lactis Probio-M8 improves bone metabolism in patients with postmenopausal osteoporosis, possibly by modulating the gut microbiota. *European Journal of Nutrition* (2022). https://doi.org/10.1007/s00394-022-03042-3

21 Sun, Y. *et al.* Probiotic Bifidobacterium animalis ssp. lactis Probio-M8 improves the fermentation and probiotic properties of fermented milk. *Journal of Dairy Science* (2024). https://doi.org/10.3168/jds.2024-24863

22 Hao, Y. *et al.* Metabolic dynamics of fermented milk beverages co-fermented with Bifidobacterium animalis subsp. lactis Probio-M8 and Lacticaseibacillus paracasei PC-01 during storage. *LWT - Food Science and Technology* (2023). https://doi.org/10.1016/j.lwt.2023.115196

23 Chen, Y. P., Hsu, C. A., Hung, W. T. & Chen, M. J. Effects ofLactobacillus paracasei01 fermented milk beverage on protection of intestinal epithelial cellin vitro. *Journal of the Science of Food and Agriculture* (2015). https://doi.org/10.1002/jsfa.7331

24 Feng, C. *et al.* Heat-Killed Bifidobacterium bifidum B1628 May Alleviate Dextran Sulfate Sodium-Induced Colitis in Mice, and the Anti-Inflammatory Effect Is Associated with Gut Microbiota Modulation. *Nutrients* (2022). https://doi.org/10.3390/nu14245233

25 Kim, W.-K. *et al.* Alleviation of DSS-induced colitis via Lactobacillus acidophilus treatment in mice. *Food & Function* (2020). https://doi.org/10.1039/d0fo01724h

26 Song, W. *et al.* Characterization of Eurotium cristatum Fermented Thinned Young Apple and Mechanisms Underlying Its Alleviating Impacts on Experimental Colitis. *Journal of Agricultural and Food Chemistry* (2024). https://doi.org/10.1021/acs.jafc.4c02005

27 Tu, J.-B., Liao, W.-J., Long, S.-P., Li, M.-P. & Gao, X.-H. Construction and validation of a machine learning model for the diagnosis of juvenile idiopathic arthritis based on fecal microbiota. *Frontiers in Cellular and Infection Microbiology* (2024). https://doi.org/10.3389/fcimb.2024.1371371

28 Blanco-Míguez, A. *et al.* Extending and improving metagenomic taxonomic profiling with uncharacterized species using MetaPhlAn 4. *Nature Biotechnology* (2023). https://doi.org/10.1038/s41587-023-01688-w

29 Chen, P. *et al.* Interaction Between Functionally Activate Endometrial Microbiota and Host Gene Regulation in Endometrial Cancer. *Frontiers in Cell and Developmental Biology* (2021). https://doi.org/10.3389/fcell.2021.727286

30 Rasmussen, J. A. *et al.* A multi-omics approach unravels metagenomic and metabolic alterations of a probiotic and synbiotic additive in rainbow trout (Oncorhynchus mykiss). *Microbiome* (2022). https://doi.org/10.1186/s40168-021-01221-8

31 Navarro-Reig, M., Jaumot, J., García-Reiriz, A. & Tauler, R. Evaluation of changes induced in rice metabolome by Cd and Cu exposure using LC-MS with XCMS and MCR-ALS data analysis strategies. *Analytical and Bioanalytical Chemistry* (2015). https://doi.org/10.1007/s00216-015-9042-2

32 Want, E. J. *et al.* Global metabolic profiling of animal and human tissues via UPLC-MS. *Nature Protocols* (2013). https://doi.org/10.1038/nprot.2012.135

33 Han, X. *et al.* A fast and accurate way to determine short chain fatty acids in mouse feces based on GC–MS. *Journal of Chromatography B* (2018). https://doi.org/10.1016/j.jchromb.2018.09.013

34 Hsu, Y.-L. *et al.* Evaluation and Optimization of Sample Handling Methods for Quantification of Short-Chain Fatty Acids in Human Fecal Samples by GC-MS. *Journal of Proteome Research* (2019). https://doi.org/10.1021/acs.jproteome.8b00536

35 Zhang, S., Wang, H. & Zhu, M.-J. A sensitive GC/MS detection method for analyzing microbial metabolites short chain fatty acids in fecal and serum samples. *Talanta* (2018). https://doi.org/10.1016/j.talanta.2018.12.049

36 Chen, G.-y., Zhong, W., Zhou, Z. & Zhang, Q. Simultaneous determination of tryptophan and its 31 catabolites in mouse tissues by polarity switching UHPLC-SRM-MS. *Analytica Chimica Acta* (2018). https://doi.org/10.1016/j.aca.2018.02.026

37 Sadok, I., Rachwał, K. & Staniszewska, M. Application of the optimized and validated LC–MS method for simultaneous quantification of tryptophan metabolites in culture medium from cancer cells. *Journal of Pharmaceutical and Biomedical Analysis* (2019). https://doi.org/10.1016/j.jpba.2019.112805

38 Alves, E., Gregório, J., Rijo, P., Rosado, C. & Monteiro Rodrigues, L. Kefir and the Gut–Skin Axis. *International Journal of Environmental Research and Public*

Health (2022). https://doi.org/10.3390/ijerph192113791

39 Li, Y. *et al.* Formation Mechanism and Nutritional Effects of Organic Acids in Fermented Foods: A Review. *Journal of Food Science* (2025). https://doi.org/10.1111/1750-3841.70745

40 Toschi, A., Rossi, B., Tugnoli, B., Piva, A. & Grilli, E. Nature-Identical Compounds and Organic Acids Ameliorate and Prevent the Damages Induced by an Inflammatory Challenge in Caco-2 Cell Culture. *Molecules* (2020). https://doi.org/10.3390/molecules25184296

41 Wang, J. *et al.* Blend of organic acids and medium chain fatty acids prevents the inflammatory response and intestinal barrier dysfunction in mice challenged with enterohemorrhagic Escherichia coli O157:H7. *International Immunopharmacology* (2018). https://doi.org/10.1016/j.intimp.2018.03.014

42 Yang, R. *et al.* Propionic Acid Targets the TLR4/NF-κB Signaling Pathway and Inhibits LPS-Induced Intestinal Barrier Dysfunction: In Vitro and In Vivo Studies. *Frontiers in Pharmacology* (2020). https://doi.org/10.3389/fphar.2020.573475

43 Chen, Y. *et al.* Indole-3-propionic acid alleviates intestinal epithelial cell injury via regulation of the TLR4/NF-κB pathway to improve intestinal barrier function. *Molecular Medicine Reports* (2024). https://doi.org/10.3892/mmr.2024.13313

44 Zhang, S., Huang, Y., Li, Y., Wang, Y. & He, X. Anti-neuroinflammatory and antioxidant phenylpropanoids from Chinese olive. *Food Chemistry* (2019). https://doi.org/10.1016/j.foodchem.2019.02.031

45 Cai, X.-X. *et al.* A comprehensive review of small molecules, targets, and pathways in ulcerative colitis treatment. *European Journal of Medicinal Chemistry* (2025). https://doi.org/10.1016/j.ejmech.2025.117645

46 Zhang, S., Huang, Y., Li, Y., Wang, Y. & He, X. Camel milk and fermented camel milk prevent dextran sulfate sodium-induced ulcerative colitis via the intestinal flora-short-chain fatty acids-mucosal barrier axis in mice. *Frontiers in Microbiology* (2025).

47 Pradhan, D. *et al.* Postbiotic Lipoteichoic acid of probiotic Lactobacillus origin ameliorates inflammation in HT-29 cells and colitis mice. *International Journal of Biological Macromolecules* (2023). https://doi.org/10.1016/j.ijbiomac.2023.123962

48 Lee, S. *et al.* Peptidoglycan from Bifidobacterium adolescentis enhances IL-10 production in regulatory B cells to alleviate gut inflammation. *Gut Microbes* (2026). https://doi.org/10.1080/19490976.2025.2611603

49 Allela, O. Q. B. *et al.* Overview of the immunomodulatory role of bacterial probiotic-derived peptidoglycan: from molecular insights to therapeutic application. *Frontiers in Microbiology* (2026). https://doi.org/10.3389/fmicb.2026.1761985

50 Neurath, M. F. Strategies for targeting cytokines in inflammatory bowel disease. *Nature Reviews Immunology* (2024). https://doi.org/10.1038/s41577-024-01008-6

51 Waldner, M. J. & Neurath, M. F. Master regulator of intestinal disease: IL-6 in chronic inflammation and cancer development. *Seminars in Immunology* (2014).

https://doi.org/10.1016/j.smim.2013.12.003
52 Niu, Y. *et al.* Targeting the intestinal circadian clock by meal timing ameliorates gastrointestinal inflammation. *Cellular & Molecular Immunology* (2024). https://doi.org/10.1038/s41423-024-01189-z
53 Neumann, C., Scheffold, A. & Rutz, S. Functions and regulation of T cell-derived interleukin-10. *Seminars in Immunology* (2019). https://doi.org/10.1016/j.smim.2019.101344
54 Woznicki, J. A. *et al.* TNF-α synergises with IFN-γ to induce caspase-8-JAK1/2-STAT1-dependent death of intestinal epithelial cells. *Cell Death & Disease* (2021). https://doi.org/10.1038/s41419-021-04151-3
55 Wu, X. *et al.* P2RY13 Exacerbates Intestinal Inflammation by Damaging the Intestinal Mucosal Barrier via Activating IL-6/STAT3 Pathway. *International Journal of Biological Sciences* (2022). https://doi.org/10.7150/ijbs.74304
56 Kaminsky, L. W., Al-Sadi, R. & Ma, T. Y. IL-1β and the Intestinal Epithelial Tight Junction Barrier. *Frontiers in Immunology* (2021). https://doi.org/10.3389/fimmu.2021.767456
57 Rawat, M. *et al.* IL1B Increases Intestinal Tight Junction Permeability by Up-regulation of MIR200C-3p, Which Degrades Occludin mRNA. *Gastroenterology* (2020). https://doi.org/10.1053/j.gastro.2020.06.038
58 Alizadeh, A., Akbari, P., Garssen, J., Fink-Gremmels, J. & Braber, S. Epithelial integrity, junctional complexes, and biomarkers associated with intestinal functions. *Tissue Barriers* (2021). https://doi.org/10.1080/21688370.2021.1996830
59 Candelli, M. *et al.* Interaction between Lipopolysaccharide and Gut Microbiota in Inflammatory Bowel Diseases. *International Journal of Molecular Sciences* (2021). https://doi.org/10.3390/ijms22126242
60 Violi, F., Pignatelli, P., Castellani, V., Carnevale, R. & Cammisotto, V. Gut dysbiosis, endotoxemia and clotting activation: A dangerous trio for portal vein thrombosis in cirrhosis. *Blood Reviews* (2022). https://doi.org/10.1016/j.blre.2022.100998
61 Zhou, C. *et al.* Ganjiang Huangqin Huanglian Renshen Decoction protects against ulcerative colitis by modulating inflammation, oxidative stress, and gut microbiota. *Phytomedicine* (2024). https://doi.org/10.1016/j.phymed.2024.156172
62 Zhang, Z. *et al.* PEAK1 maintains tight junctions in intestinal epithelial cells and resists colitis by inhibiting autophagy-mediated ZO-1 degradation. *Nature Communications* (2025). https://doi.org/10.1038/s41467-025-62107-z
63 Yao, D., Dai, W., Dong, M., Dai, C. & Wu, S. MUC2 and related bacterial factors: Therapeutic targets for ulcerative colitis. *EBioMedicine* (2021). https://doi.org/10.1016/j.ebiom.2021.103751
64 Qiao, Y., He, C., Xia, Y., Ocansey, D. K. W. & Mao, F. Intestinal mucus barrier: A potential therapeutic target for IBD. *Autoimmunity Reviews* (2024). https://doi.org/10.1016/j.autrev.2024.103717
65 Zhu, L. *et al.* Stanniocalcin-1 Promotes PARP1-Dependent Cell Death via JNK

Activation in Colitis. *Advanced Science* (2023). https://doi.org/10.1002/advs.202304123

66 Bastaki, S. M. A., Amir, N., Adeghate, E. & Ojha, S. Lycopodium Mitigates Oxidative Stress and Inflammation in the Colonic Mucosa of Acetic Acid-Induced Colitis in Rats. *Molecules* (2022). https://doi.org/10.3390/molecules27092774

67 Su, P. *et al.* The antioxidant activity of polysaccharides from Armillaria gallica. *Frontiers in Nutrition* (2024). https://doi.org/10.3389/fnut.2024.1277877

68 Henneke, L. *et al.* A dietary carbohydrate – gut Parasutterella – human fatty acid biosynthesis metabolic axis in obesity and type 2 diabetes. *Gut Microbes* (2022). https://doi.org/10.1080/19490976.2022.2057778

69 Ju, T., Kong, J. Y., Stothard, P. & Willing, B. P. Defining the role of Parasutterella, a previously uncharacterized member of the core gut microbiota. *The ISME Journal* (2019). https://doi.org/10.1038/s41396-019-0364-5

70 Deretic, V., Saitoh, T. & Akira, S. Autophagy in infection, inflammation and immunity. *Nature Reviews Immunology* (2013). https://doi.org/10.1038/nri3532

71 Virgin, H. W. & Levine, B. Autophagy genes in immunity. *Nature Immunology* (2009). https://doi.org/10.1038/ni.1726

72 Deretic, V. & Levine, B. Autophagy balances inflammation in innate immunity. *Autophagy* (2018). https://doi.org/10.1080/15548627.2017.1402992

73 Tillett, B. J. *et al.* SCFA biotherapy delays diabetes in humanized gnotobiotic mice by remodeling mucosal homeostasis and metabolome. *Nature Communications* (2025). https://doi.org/10.1038/s41467-025-58319-y

74 Yang, Y. *et al.* Bupleuri Radix Polysaccharides Alleviate MASLD by Regulating Muribaculaceae-Derived SCFAs in the Gut–Liver Axis. *International Journal of Molecular Sciences* (2026). https://doi.org/10.3390/ijms27020637

75 Zhang, Y. *et al.* Intestinal organoid screen reveals that Bacillus velezensis PGM541 promotes epithelial proliferation via its metabolite butyric acid. *Microbiome* (2026). https://doi.org/10.1186/s40168-026-02346-4

76 Xue, C. *et al.* Tryptophan metabolism in health and disease. *Cell Metabolism* (2023). https://doi.org/10.1016/j.cmet.2023.06.004

77 Stone, T. W. & Williams, R. O. Modulation of T cells by tryptophan metabolites in the kynurenine pathway. *Trends in Pharmacological Sciences* (2023). https://doi.org/10.1016/j.tips.2023.04.006

78 Michaudel, C. *et al.* Rewiring the altered tryptophan metabolism as a novel therapeutic strategy in inflammatory bowel diseases. *Gut* (2023). https://doi.org/10.1136/gutjnl-2022-327337

79 Wang, Z. *et al.* FUT2-dependent fucosylation of HYOU1 protects intestinal stem cells against inflammatory injury by regulating unfolded protein response. *Redox Biology* (2023). https://doi.org/10.1016/j.redox.2023.102618

80 Li, W. *et al.* L-fucose and fucoidan alleviate high-salt diet-promoted acute inflammation. *Frontiers in Immunology* (2024). https://doi.org/10.3389/fimmu.2024.1333848

81 Zhang, X. *et al.* Taxifolin attenuates inflammation via suppressing MAPK signal

pathway in vitro and in silico analysis. *Chinese herbal medicines* (2022). https://doi.org/10.1016/j.chmed.2021.03.002

82 Althunibat, O. Y., Abukhalil, M. H., Khwaldeh, A., Abu-Zaiton, A. & Al-fawaeir, S. Protective effects of taxifolin against gentamicin-induced nephrotoxicity in mice: modulation of oxidative stress, inflammation, apoptosis, and Nrf2 signaling. *Naunyn-Schmiedeberg's Archives of Pharmacology* (2025). https://doi.org/10.1007/s00210-025-04396-1

83 Nowacka, A., Śniegocki, M., Śniegocka, M. & Ziółkowska, E. A. Nicotinamide and Pyridoxine in Muscle Aging: Nutritional Regulation of Redox, Inflammation, and Regeneration. *Antioxidants* (2025). https://doi.org/10.3390/antiox14080911

84 Jaruan, O. *et al.* Pyridoxine exerts antioxidant effects on kidney injury manifestations in high-fat diet-induced obese rats. *Chemico-Biological Interactions* (2025). https://doi.org/10.1016/j.cbi.2025.111513

85 Han, E.-J. *et al.* (–)-Loliolide Isolated from Sargassum horneri Suppressed Oxidative Stress and Inflammation by Activating Nrf2/HO-1 Signaling in IFN-γ/TNF-α-Stimulated HaCaT Keratinocytes. *Antioxidants* (2021). https://doi.org/10.3390/antiox10060856

86 Leung, H. K. M. *et al.* Zearalenone attenuates colitis associated colorectal tumorigenesis through Ras/Raf/ERK pathway suppression and SCFA-producing bacteria promotion. *Biomedicine & Pharmacotherapy* (2023). https://doi.org/10.1016/j.biopha.2023.114973

87 Sun, X., Yang, Q., Rogers, C. J., Du, M. & Zhu, M.-J. AMPK improves gut epithelial differentiation and barrier function via regulating Cdx2 expression. *Cell Death and Differentiation* (2017). https://doi.org/10.1038/cdd.2017.14

88 McBride, D. A. *et al.* Short-chain fatty acid-mediated epigenetic modulation of inflammatory T cells in vitro. *Drug Delivery and Translational Research* (2022). https://doi.org/10.1007/s13346-022-01284-6

89 Pyun, D. H. *et al.* Endogenous metabolite, kynurenic acid, attenuates nonalcoholic fatty liver disease via AMPK/autophagy- and AMPK/ORP150-mediated signaling. *Journal of Cellular Physiology* (2020). https://doi.org/10.1002/jcp.30199

90 Stone, T. W., Darlington, L. G., Badawy, A. A. B. & Williams, R. O. The Complex World of Kynurenic Acid: Reflections on Biological Issues and Therapeutic Strategy. *International Journal of Molecular Sciences* (2024). https://doi.org/10.3390/ijms25169040

91 Li, Q., Chen, H., Zhang, M., Wu, T. & Liu, R. Altered short chain fatty acid profiles induced by dietary fiber intervention regulate AMPK levels and intestinal homeostasis. *Food & Function* (2019). https://doi.org/10.1039/c9fo01465a

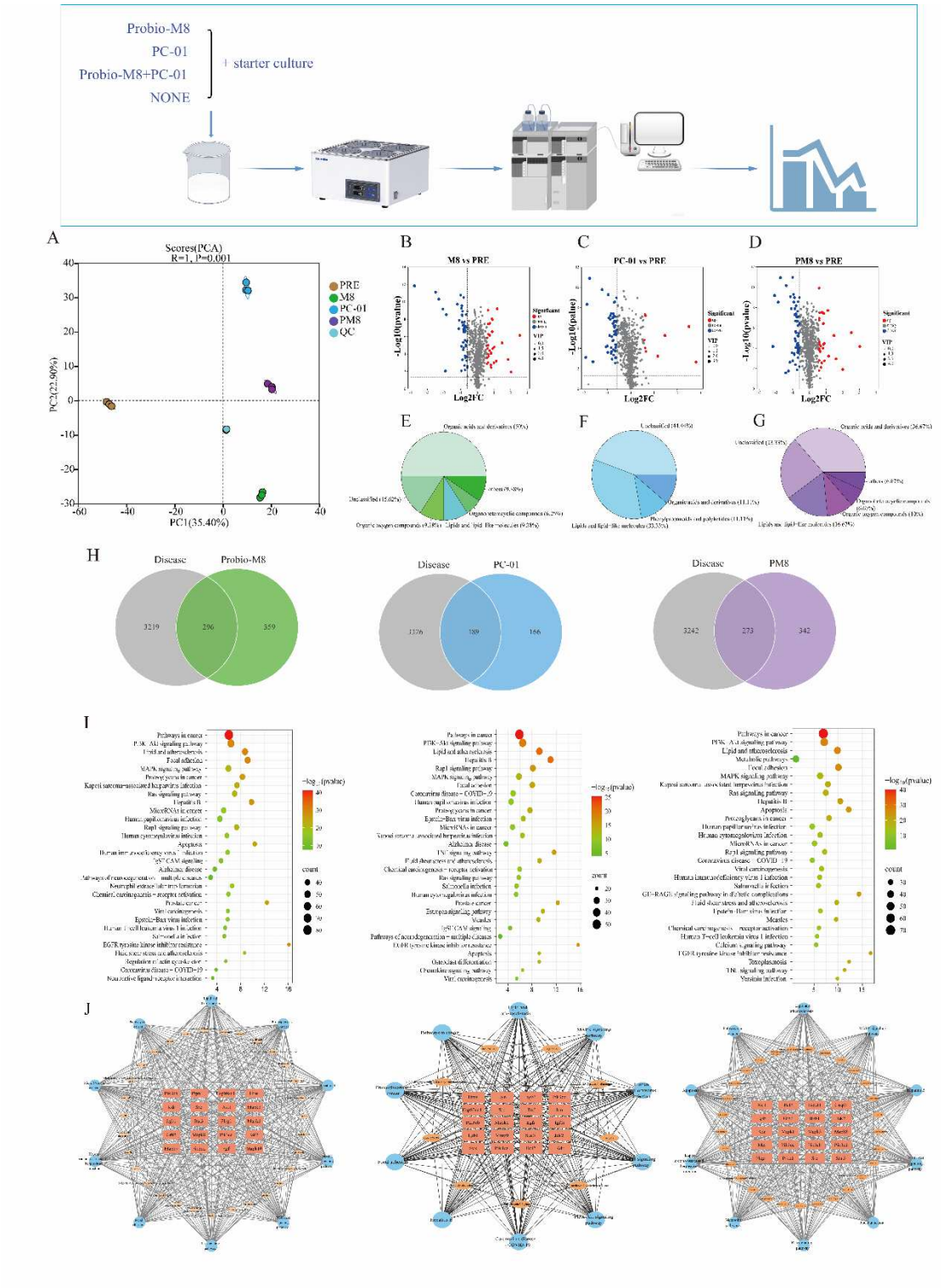


Figure. 1.Preparation of pasteurized fermented milk and analysis of fermented milk metabolites and disease-related activity. (A) PCA score plot of fermented milk in each group. (B) Volcano plot of differential metabolites between Probio-M8 pasteurized fermented milk and ordinary

pasteurized fermented milk. (C) Volcano plot of differential metabolites between PC-01 pasteurized fermented milk and ordinary pasteurized fermented milk. (D) Volcano plot of differential metabolites between PM8 combined pasteurized probiotic fermented milk and ordinary pasteurized fermented milk. (E–G) Pie charts showing classification of differential metabolites between Probio-M8, PC-01, and PM8 pasteurized fermented milk and PRE fermented milk, respectively. (H) Venn diagram of overlapping targets between differential metabolite targets and disease targets for the three pasteurized probiotic fermented milk products. (I) KEGG enrichment pathways of common targets between differential metabolites and diseases for the three pasteurized probiotic fermented milk products. (J) Compound-target-pathway networks corresponding to the three pasteurized probiotic fermented milk products. Data are presented as mean ± SD. PRE, pasteurized fermented milk without probiotic addition; M8, Probio-M8 pasteurized fermented milk; PC-01, PC-01 pasteurized fermented milk; PM8, combined pasteurized fermented milk with Probio-M8 and PC-01.

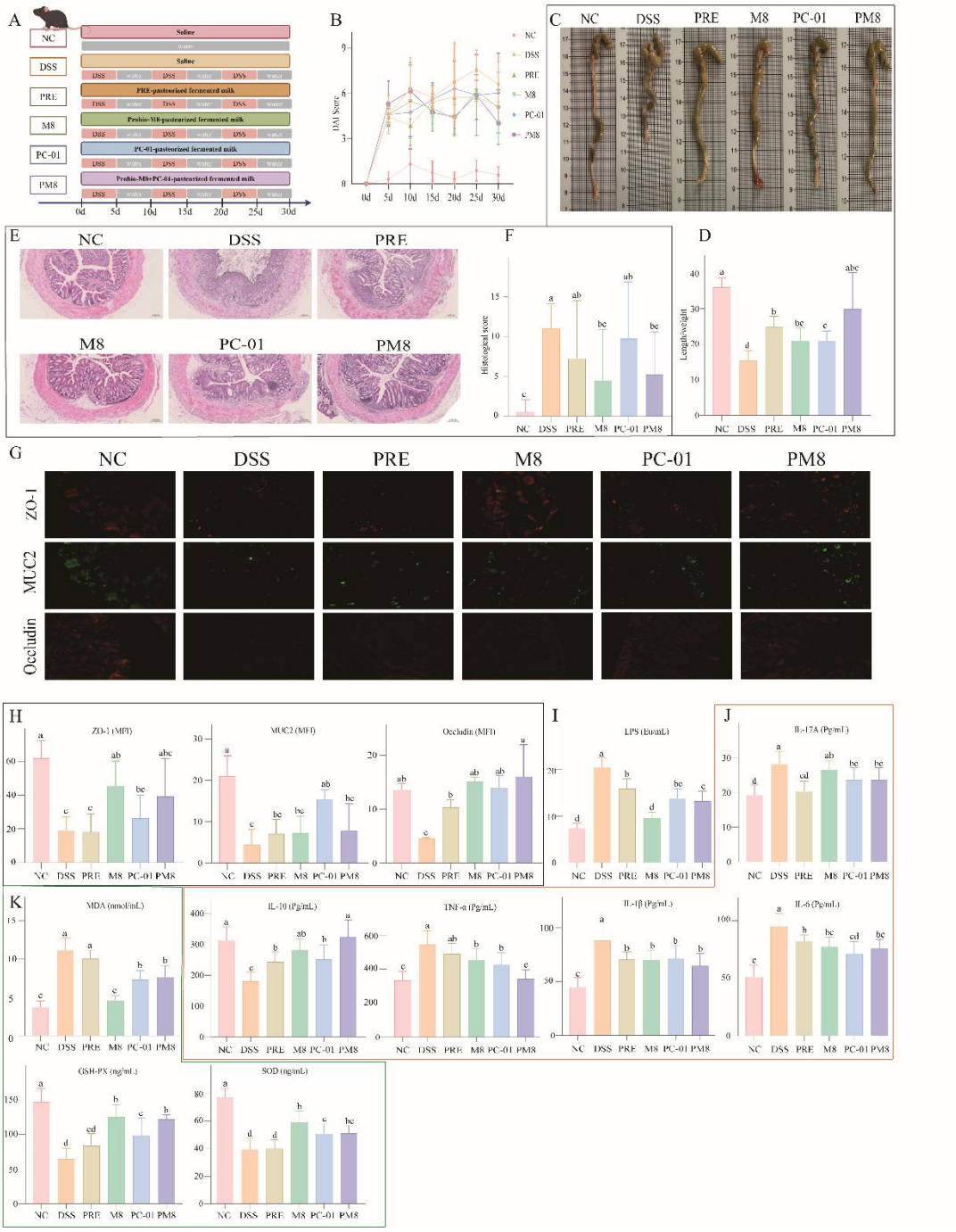


Figure. 2. Pasteurized fermented milk ameliorates DSS-induced colitis symptoms in mice. (A) Schematic diagram of the animal experimental design. (B) DAI scores. (C) Representative images of colons. (D) Colon length-to-weight ratio. (E) Representative histopathological images of colon sections (10×). (F) Histological scores (n=4). (G) Representative immunofluorescence images of ZO-1, MUC2, and occludin (40×).. (H) Protein expression levels of ZO-1, MUC2, and Occludin (n=3). (I) Serum LPS levels. (J) Serum levels of IL-17A, IL-6, IL-1β, TNF-α, and IL-10. (K) Serum levels of MDA, SOD, and GSH-PX. Data are presented as mean ± SD. The colon length-to-weight ratio was analyzed using the Wilcoxon rank-sum test, and all other parameters were analyzed using t-test. Statistical significance is

indicated by letters. NC, normal control group; DSS, model group with intermittent 2.5% DSS in drinking water; PRE, group gavaged with 0.2 mL/day pasteurized fermented milk without probiotic addition combined with intermittent 2.5% DSS in drinking water; M8, group gavaged with 0.2 mL/day pasteurized probiotic fermented milk containing Probio-M8 combined with intermittent 2.5% DSS in drinking water; PC-01, group gavaged with 0.2 mL/day pasteurized probiotic fermented milk containing PC-01 combined with intermittent 2.5% DSS in drinking water; PM8, group gavaged with 0.2 mL/day pasteurized probiotic fermented milk containing both Probio-M8 and PC-01 combined with intermittent 2.5% DSS in drinking water.

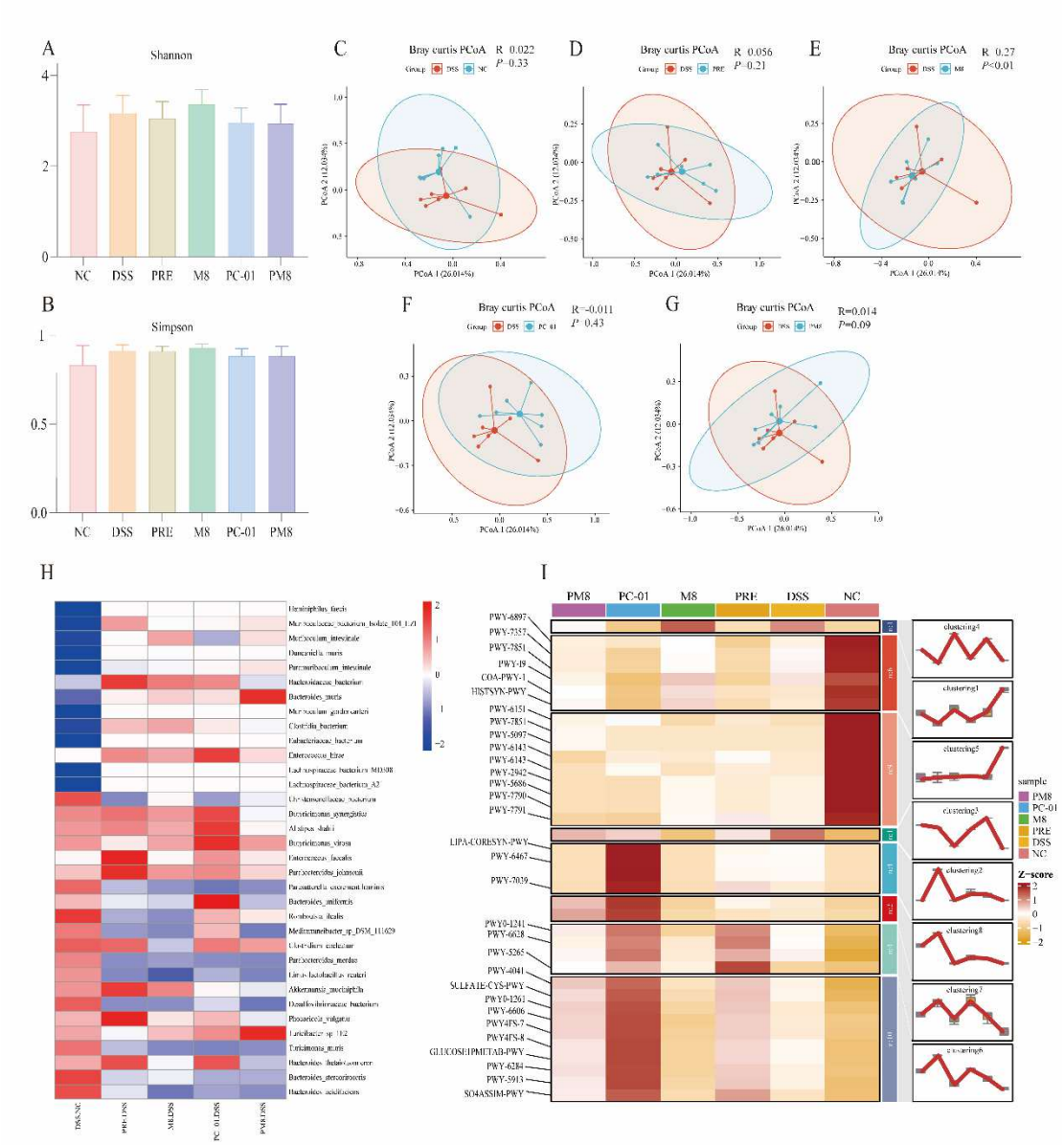


Figure. 3**.** Pasteurized fermented milk restores DSS-induced gut microbiota dysbiosis. (A, B) Alpha diversity expressed as Shannon and Simpson indices. (C–G) Beta diversity of gut

microbiota between the DSS and NC groups, and between the DSS group and the PRE, M8, PC-01, and PM8 groups, respectively, shown by PCoA and Anosim. (H) Heatmap of relative abundances of key species annotated by MetaPhlan4 (Difference between two groups). (I) Trend heatmap of predicted metabolic pathways obtained from HUMAnN3. Data are presented as mean ± SD. Differences between two groups for diversity indices and bacterial species expression levels were calculated using the Wilcoxon rank-sum test. For predicted pathways, differences among groups were calculated using the Kruskal-Wallis test, and pathways with $p < 0.004$ are shown. Statistical significance is indicated by p-values. NC, normal control group; DSS, model group with intermittent 2.5% DSS in drinking water; PRE, group gavaged with 0.2 mL/day pasteurized fermented milk without probiotic addition combined with intermittent 2.5% DSS in drinking water; M8, group gavaged with 0.2 mL/day pasteurized probiotic fermented milk containing Probio-M8 combined with intermittent 2.5% DSS in drinking water; PC-01, group gavaged with 0.2 mL/day pasteurized probiotic fermented milk containing PC-01 combined with intermittent 2.5% DSS in drinking water; PM8, group gavaged with 0.2 mL/day pasteurized probiotic fermented milk containing both Probio-M8 and PC-01 combined with intermittent 2.5% DSS in drinking water.

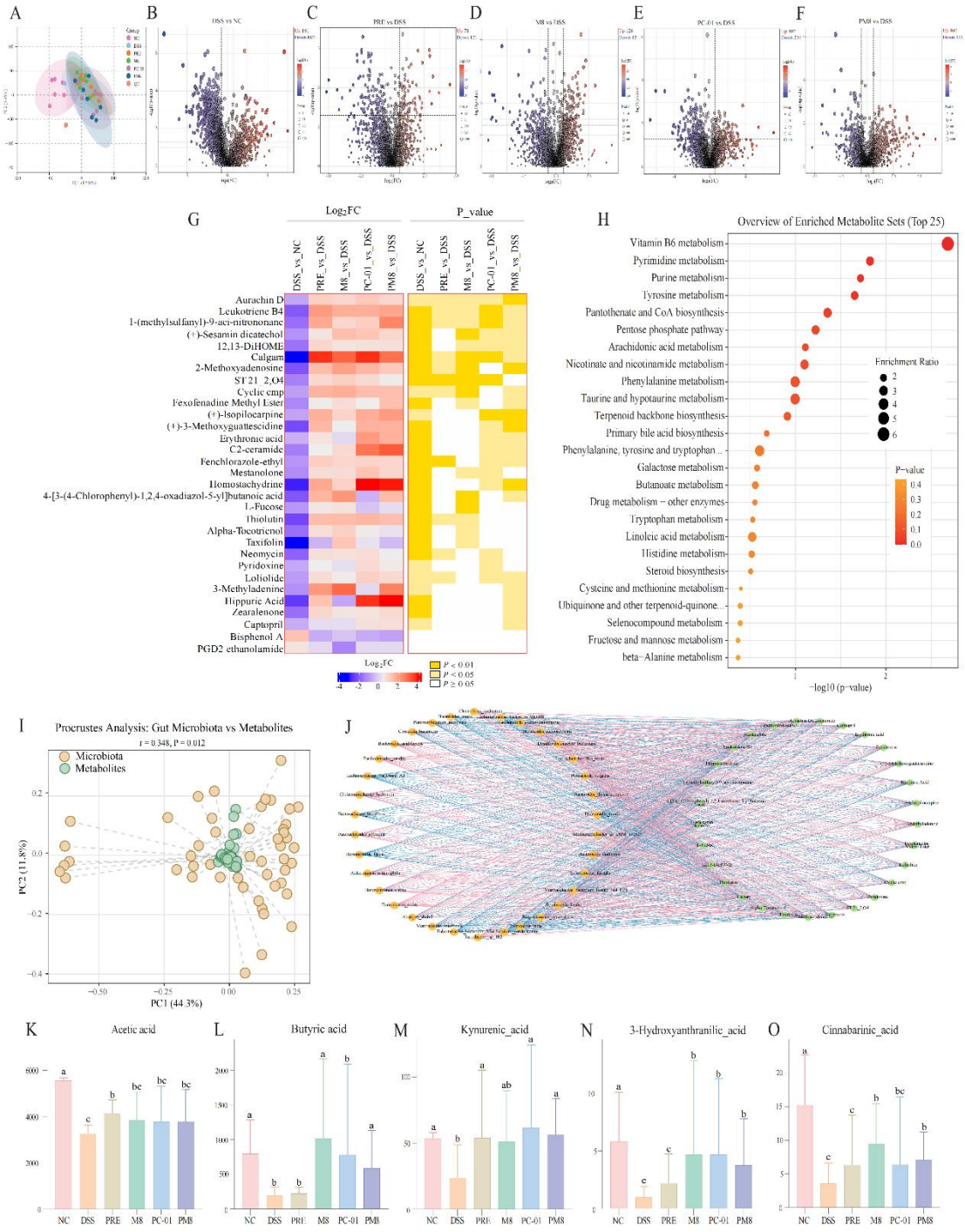


Figure. 4. Pasteurized fermented milk restores fecal metabolite contents. (A) PCA plot of metabolites in each group. (B–F) Volcano plots of DSS vs. NC, and PRE, M8, PC-01, and PM8 vs. DSS, respectively. (G) Heatmap of differential metabolites between DSS and NC, and between PRE, M8, PC-01, PM8 and DSS groups, based on FC values and p-values. (H) Metabolic pathway map corresponding to differential metabolites. (I) Procrustes analysis plot

of gut microbiota and metabolites. (J) Spearman correlation heatmap between gut microbiota and metabolites. (K) Acetic acid content (μg/g) in each group (n=3). (L) Butyric acid content (μg/g) in each group (n=3). (M) Kynurenic acid content (μg/g) in each group (n=3). (N) 3-Hydroxyanthranilic acid content (μg/g) in each group (n=3). (O) Cinnabarinic acid content (μg/g) in each group (n=3). Data are presented as mean ± SD. Differences between two groups for targeted metabolites were calculated using t-test. NC, normal control group; DSS, model group with intermittent 2.5% DSS in drinking water; PRE, group gavaged with 0.2 mL/day pasteurized fermented milk without probiotic addition combined with intermittent 2.5% DSS in drinking water; M8, group gavaged with 0.2 mL/day pasteurized probiotic fermented milk containing Probio-M8 combined with intermittent 2.5% DSS in drinking water; PC-01, group gavaged with 0.2 mL/day pasteurized probiotic fermented milk containing PC-01 combined with intermittent 2.5% DSS in drinking water; PM8, group gavaged with 0.2 mL/day pasteurized probiotic fermented milk containing both Probio-M8 and PC-01 combined with intermittent 2.5% DSS in drinking water.

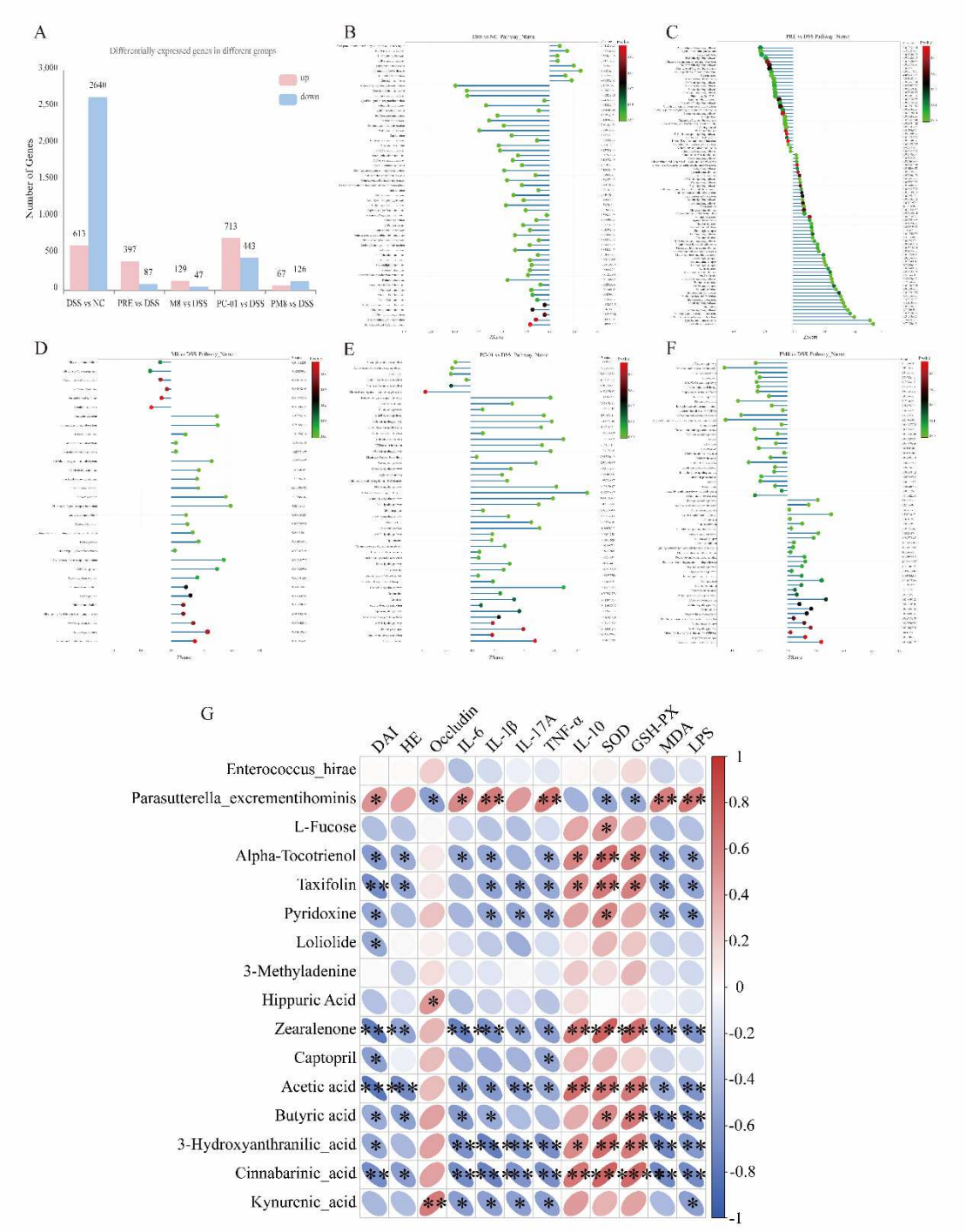


Figure. 5. Colonic transcriptomic profiles and correlation expression plots. (A) Number of differentially expressed genes between DSS and NC groups, and between PRE, M8, PC-01, PM8 and DSS groups, respectively. (B–F) Expression of differential pathways between DSS and NC groups, and between PRE, M8, PC-01, PM8 and DSS groups, respectively. (G) Correlations between basic parameters and gut microbiota as well as fecal metabolite markers in each group. Data are presented as mean ± SD. NC, normal control group; DSS, model group with intermittent 2.5% DSS in drinking water; PRE, group gavaged with 0.2 mL/day pasteurized fermented milk without probiotic addition combined with intermittent 2.5% DSS

in drinking water; M8, group gavaged with 0.2 mL/day pasteurized probiotic fermented milk containing Probio-M8 combined with intermittent 2.5% DSS in drinking water; PC-01, group gavaged with 0.2 mL/day pasteurized probiotic fermented milk containing PC-01 combined with intermittent 2.5% DSS in drinking water; PM8, group gavaged with 0.2 mL/day pasteurized probiotic fermented milk containing both Probio-M8 and PC-01 combined with intermittent 2.5% DSS in drinking water.

Supplementary Files

This is a list of supplementary files associated with this preprint. Click to download.

- Supplementary.pdf